

UNCLASSIFIED

AD 491121

DEFENSE DOCUMENTATION CENTER

FOR

SCIENTIFIC AND TECHNICAL INFORMATION

CAMERON STATION ALEXANDRIA, VIRGINIA



UNCLASSIFIED

NOTICE: When government or other drawings, specifications or other data are used for any purpose other than in connection with a definitely related government procurement operation, the U. S. Government thereby incurs no responsibility, nor any obligation whatsoever; and the fact that the Government may have formulated, furnished, or in any way supplied the said drawings, specifications, or other data is not to be regarded by implication or otherwise as in any manner licensing the holder or any other person or corporation, or conveying any rights or permission to manufacture, use or sell any patented invention that may in any way be related thereto.

SECRET

WT-1424-1

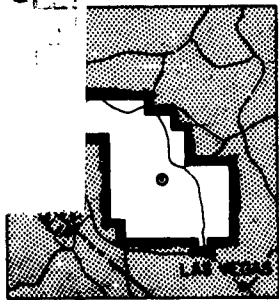


2

491121

COPY

OPERATION PLUMBBOB



NEVADA TEST SITE
MAY-OCTOBER 1957

hey

Project 3.5a

ISOLATION OF STRUCTURES FROM GROUND SHOCK

Issuance Date: April 23, 1962

HEADQUARTERS FIELD COMMAND
DEFENSE ATOMIC SUPPORT AGENCY
SANDIA BASE, ALBUQUERQUE, NEW MEXICO



491121

DDC
RECEIVED
SEP 5 1964
SEP J
DISTRIBUTION
DCC-IRA B
DL

62-05-5384

Inquiries relative to this report may be made to

**Chief, Defense Atomic Support Agency
Washington 25, D. C.**

DO NOT RETURN THIS DOCUMENT

12-14-14
19 WT 1424, 1

21
Report

WT-1424-1

OPERATION PLUMBBOB, PROJECT 3.5a,

6

ISOLATION OF STRUCTURES FROM
GROUND SHOCK,

12 →

R. B. Vaile, Jr., ~~Project Officer~~

Stanford Research Inst.,
Menlo Park, Calif.

3

This report supersedes WT-1424,
issued 18 April 1960.



ABSTRACT

The effectiveness of frangible backfill (glass bottles) in protecting underground structures from the violent motions produced by nearby explosions was investigated. Two test structures and one comparison structure were used. Each test structure was a reinforced concrete pipe enclosing a steel cylinder separated from the pipe by rubber O-rings, with glass bottles placed around the sides and bottom of the pipe. The comparison structure was a concrete pipe with solid concrete bottom. All three structures were buried with their axes vertical, and their tops approximately 2 feet below ground level. A concrete slab 1 foot thick was set above each, flush with the ground surface. One test structure and the comparison structure were 750 feet from ground zero (229-psi peak overpressure). The remaining test structure was 1,050 feet from ground zero (104-psi peak overpressure).

The peak accelerations of these structures, produced by shear forces exerted against their sides, were reduced by the frangible backfill to 26 percent or less of those that structures in intimate contact with the soil would have experienced.

Four years after the shot the structures were excavated. All the bottles around the sides of the test structure at 229 psi were completely crushed; only a fourth of the bottles at the 104-psi location were broken, most of these on the upper half of the structure.

At the 229-psi location the soil apparently was stressed beyond failure, and the protective capabilities of the backfill were fully utilized. At the 104-psi location the backfill capabilities were 10 percent expended; the configuration could have accepted a second attack at 200 psi or four or five attacks at 100 psi. ←

The soil beneath the two test structures moved down a greater distance than the structures, and the frangible elements beneath them showed no crushing and only minor fracturing.

The frangible backfill was shown to enhance the protection afforded by an underground structure against more than one attack of relatively small magnitude while retaining a major part of the capability to protect against a single large attack. Further investigation is recommended.

FOREWORD

This report presents the final results of one of the 46 projects comprising the military-effect program of Operation Plumbbob, which included 24 test detonations at the Nevada Test Site in 1957. WT-1424 was originally published in April 1960. Since then, post-operation work on the project produced additional results. WT-1424-1 contains all the information published in the original report, plus the additional results.

For overall Plumbbob military-effects information, the reader is referred to the "Summary Report of the Director, DOD Test Group (Programs 1-9)," ITR-1445, which includes: (1) a description of each detonation, including yield, zero-point location and environment, type of device, ambient atmospheric conditions, etc.; (2) a discussion of project results; (3) a summary of the objectives and results of each project; and (4) a listing of project reports for the military-effect program.

PREFACE

The successful performance of this experiment, in common with a large number of other experiments, would not have been possible without the wholehearted cooperation and assistance of many people. The Program Director, Lt Col Todd Bingham, and his office, were at all times helpful. The Waterways Experiment Station Group, under T. B. Goode, was responsible for determination of soil properties and for measurement of the moisture content of the sand used for backfill. The Reynolds Electric and Engineering Company went to great lengths, in fact, required four trials to obtain dry sand, and Field Superintendent Mr. Earl Bonney went out of his way on many occasions to assist the project. The design of the cover slabs, complete with manhole covers, was the responsibility of Holmes and Narver, Inc., and the results were fully satisfactory. John Case, Consulting Structural Engineer, designed the structures and assisted with great effectiveness in taking the field measurements and interpreting the results. The American Pipe and Construction Company paid special attention to the construction of the structures and met shipping schedules in a satisfactory fashion. The Gilbey Division of the National Distillers Corporation and the Internal Revenue Bureau, both in San Francisco and in Washington, were fully cooperative in permitting and supplying the desired frangible elements.

Stanford Research Institute's participation in this project was as follows: Mr. W. M. Wells and Dr. R. B. Vaile, Jr. were responsible for the general direction. The project was handled as one of many tasks undertaken during Operation Plumbbob by the Instrumentation Group under the broad direction of Mr. L. M. Swift and Mr. L. H. Inman. The members of the group were R. E. Aumiller, V. E. Krakow, R. V. Ohler, C. M. Westbrook, and H. Wuner.

The excavation party was led by Dr. R. B. Vaile, Jr. Included in the group were Mr. John Case, Mr. William Wells, Mr. Richard Ohler, and Miss Phyllis Flanders. Dr. G. N. Bycroft of Stanford Research Institute, Dr. R. V. Whitman of Massachusetts Institute of Technology, and Mr. John Case assisted in the analysis of the excavation results.

In the excavation of the structures, the interested and effective collaboration of CDR H. L. Murphy, Field Command, Defense Atomic Support Agency, was very much in evidence. He was especially effective in making arrangements necessary to the excavation procedure and in calibration of the beams to support the structures during the excavation.

CONTENTS

ABSTRACT -----	5
FOREWORD -----	6
PREFACE -----	6
CHAPTER 1 INTRODUCTION -----	11
1.1 Objective-----	11
1.2 Background -----	11
1.3 Theory -----	12
CHAPTER 2 PROCEDURE -----	14
2.1 Design of Structure-----	14
2.2 Design of Special Backfill-----	14
2.3 Instrumentation -----	16
2.4 Excavation-----	16
CHAPTER 3 RESULTS AND DISCUSSION -----	27
3.1 Acceleration -----	27
3.2 Velocity -----	28
3.3 Displacement-----	29
3.4 Excavation-----	32
3.4.1 Structure 3 -----	32
3.4.2 Structure 1 -----	33
3.5 Some Theoretical Considerations of Bottle Breakage-----	33
3.5.1 Volume Change of Unsupported Elastic Hole -----	34
3.5.2 Soil Mechanics Approach -----	35
3.6 Summary of Results -----	37
CHAPTER 4 MULTIPLE-ATTACK PROBLEM -----	60
CHAPTER 5 CONCLUSIONS AND RECOMMENDATIONS -----	64
5.1 Conclusions -----	64
5.2 Recommendations -----	65
REFERENCES -----	66
TABLES	
3.1 Structure Motion Compared with Free-Field Motion, Peak Values-----	38
3.2 Relative Permanent Horizontal Displacements of Structures-----	39
3.3 Permanent Vertical Displacements of Slabs-----	39

3.4 Relative Displacements as Shown by Scratch Gages and Cork-and-String Gages -----	39
---	----

FIGURES

2.1 Comparison structure and test structure-----	18
2.2 Cross section of inner and outer cylinders, test structures -----	19
2.3 Reinforced-concrete pipe, outer cylinder -----	20
2.4 Test structure and frangible elements in place in hole-----	20
2.5 Frangible elements around outer cylinder of test structure -----	20
2.6 Plan and elevation views of base for inner cylinder-----	21
2.7 Plan and elevation views of base for outer cylinder-----	21
2.8 Inner cylinder base -----	22
2.9 Outer cylinder base-----	22
2.10 Bases for inner and outer cylinders, assembled -----	22
2.11 Concrete slab and hatch cover, in place -----	22
2.12 Details of concrete slab and hatch cover -----	23
2.13 Cross section of test structure in place-----	24
2.14 Structure locations -----	24
2.15 Interior, Structure 3, showing scratch gages and cork-and-string gages -----	25
2.16 Support scheme for structure during excavation, Structure 3 -----	25
2.17 Excavating party at work, Structure 1-----	26
3.1 Ground and structure acceleration at 229-psi surface overpressure level-----	40
3.2 Ground and structure acceleration at 104-psi surface overpressure level-----	41
3.3 Ground and structure velocity at 229-psi surface overpressure level-----	42
3.4 Ground and structure velocity at 104-psi surface overpressure level-----	43
3.5 Ground and structure displacement at 229-psi surface overpressure level-----	44
3.6 Ground and structure displacement at 104-psi surface overpressure level-----	45
3.7 Comparison of relative displacements in Structure 1-----	46
3.8 Comparison of relative displacements, outer and inner cylinders, Structure 1 -----	47
3.9 Scratch gage record, Structure 2-----	47
3.10 Comparison of relative displacements in Structure 3-----	47
3.11 Developed surface of excavated Structure 3 indicating condition of bottles -----	49
3.12 Structure 3 during excavation -----	50
3.13 Additional views of Structure 3 during excavation -----	51
3.14 View of Structure 3 showing lateral movement that occurred during excavation -----	52
3.15 Subbase of Structure 3 -----	52
3.16 Inner subbase of Structure 3 exposed -----	52
3.17 Top of Structure 1 as excavated-----	53
3.18 Typical condition of bottles attached to Structure 1 -----	54
3.19 View showing bottles in lower part of Structure 1 -----	55
3.20 View of lower part of Structure 1 showing offset, which occurred during placement, and water damage-----	55
3.21 Bottom of Structure 1 and subbase showing displaced O-ring-----	56
3.22 Inner subbase of Structure 1 exposed -----	57

3.23	Lateral stress as a function of vertical stress -----	58
3.24	Diagram of failure wedge -----	59
4.1	Overpressure and probability as a function of radius-----	62
4.2	Probability versus overpressure -----	63

Chapter 1

INTRODUCTION

1.1 OBJECTIVE

The overall objective was to make an initial study of the benefit derived from special backfills in isolating or protecting underground structures and their contents from the physical effects of explosions. The immediate objective was to test the value of two specific forms of special backfill, namely, frangible elements and shear barriers.

1.2 BACKGROUND

The primary function of an underground structure is to protect its contents from the effects of ground motion resulting from underground, surface, and aboveground explosions. From the considerable information on the general topic of damage to underground structures, particularly damage from underground explosions, it seems clear that there is a need for improvement in the protection provided by underground structures against ground motion effects. One way to achieve this is to use a specially designed backfill around the structure to absorb the energy and reduce the forces otherwise incident on it. As far as is known, this concept was not tested until Operation Plumbbob (1957), although it was indicated in a test planning meeting held by the Armed Forces Special Weapons Project (AFSWP), 24 May 1956, that special backfills had been thought of and discussed by a number of people many months earlier than the meeting.

As a part of Operation Plumbbob, a specially designed frangible backfill placed around buried structures (concrete cylinders) was tested during Shot Priscilla (36.6 kt; height of burst: 700 feet (balloon); 24 June 1957). After Priscilla, the structures were not excavated immediately to determine by observation the portion of the backfill that was destroyed and to estimate the degree of protection remaining in the frangible elements. The excavation was delayed in the hope that another test shot could be fired over the structures; in such a case, the information on the capability of the protected structures to withstand multiple shots would have been of more value than the information gained by excavation. In the intervening years, the climate for testing changed to the extent that it was unlikely that an aboveground nuclear shot would ever again be fired on Frenchman Flat. Therefore, in 1960, it was decided to excavate the structures when the weather at Nevada Test Site and concurrent commitments to the Defense Atomic Support Agency (DASA, formerly AFSWP) permitted. The concrete slabs over the cylinders were removed in early November 1960, and in April 1961 the excavation was completed.

This report discusses the initial plans and construction prior to the test, the test itself, the results of the data collected at that time together with the results of the excavation, and finally a review of the entire topic from the point of view of its significance to the design of underground protective structures.

1.3 THEORY

Structures can probably be built sufficiently strong so that when even large forces are applied to them they will remain intact, although their contents are damaged by the accelerations, and the necessary entrances for personnel, materiel, communications, and power are damaged or destroyed by differential movement. To minimize in particular the acceleration of the contents of a structure, it is desirable to study means of isolation of a structure from its surroundings.

The designer of a full-scale structure intended to resist the effects of actual explosions cannot possibly foretell the exact magnitude of the explosion that the structure must withstand nor the burst point. For this reason, the designer accepts, or imposes on himself, some essentially arbitrary limits of explosion size and distance. In addition, the designer must consider the principle that, as the input loads on the structure become larger and larger, the failure of the structure should not be a sudden total collapse. Adherence to this principle forbids, for example, a structure to be isolated simply by the provision of a continuous void around the sides of the structure. (If this were done, the structure would receive no load from inputs that represent less maximum deflection than the void provided but would receive severe loads for all inputs exceeding this value.) Adherence to this principle also suggests that a structure whose resistance increases as its deflections move into the plastic range will be superior to a similar structure that is brittle.

An underground explosion exerts primarily radial horizontal forces on shallow underground structures near the explosion but outside the crater. These forces combine as a linear acceleration and as a crushing force. Protection in the form of isolation for such a structure should probably consist of frangible material in the backfill around the sides, and shear barriers at the top and bottom of the structure.

An aboveground explosion produces on shallow underground structures forces that are primarily vertical. Thus, protection in the form of isolation for such structures would involve frangible backfill above the top and below the bottom and shear barriers at the sides.

Obviously, if an underground structure is to be isolated from both aboveground and underground explosions, both shear barriers and frangible backfill should be applied on all sides and on the top and bottom.

Frangible backfill is conceived to be many relatively small volumes that will withstand the ordinary static foundation pressures without deflection or creep but which will fail and form voids under explosion-induced forces. It is necessary that such frangible elements be essentially watertight so that their interiors will not fill with water if ground water should rise.

A shear barrier is conceived to be any pair of surfaces that are lubricated or separated by balls or rollers so that the normal forces necessary to hold the structure in the proper position statically can be carried, but only a small fraction of the shear forces applied under explosion conditions will be transmitted between the surfaces. The requirement for use in actual construction of such shear barriers is that the antifriction properties remain effective over long periods of time. Corrosion and aging reduce the effectiveness of these antifriction properties. However, solid lubricants, such as powdered graphite, molybdenum disulfide, and the like, if applied in thick layers (for example, of the order of 1 inch), might remain effective indefinitely. On the other hand, it is doubtful that grease lubrication can be maintained effectively over long periods, because the grease will oxidize, and inevitable small vibrations will force the grease away from the points of contact.

The requirements for a test of the principle of structure isolation do not require that all the longtime characteristics desired in the frangible backfill and the shear barrier be present in the test configuration. It was the philosophy of this experiment to test the isolation principle, with only reasonable concern with the longtime properties of these devices.

The basic premise of the experiment was that, if a protected structure and an equivalent unprotected comparison structure were placed at the same radius from an explosion, the effectiveness of the protection would be indicated by the extent to which the motion of the protected test structure was smaller than that of the unprotected comparison structure.

There was an optimum radius from the explosion at which these structures should be placed. In determining the outer boundary, there were two chief considerations. One was that the structures should be placed closer to ground zero than the radius at which the explosion-induced forces were small compared with static forces exerted by the soil under no-explosion conditions. Another was that, since the frangible backfill must have a threshold of stress below which it would not break, no protection was afforded until the structures were moved toward ground zero to a point where the stresses exceeded this threshold.

The inner bound of radius for the experiment was the distance at which pressures or stresses were high enough to make prohibitively expensive the construction of structures that would withstand the crushing forces.

Normal foundation pressures for aboveground buildings are of the order of 1,000 to 4,000 psf (roughly 10 to 30 psi). For buried structures, or structures with deep foundations, the geostatic forces amount to somewhat less than 1 psi per foot of depth. These normal foundation pressures constitute a minimum threshold for the strength of frangible elements.

To maintain the experiment within reasonable bounds of cost, it was decided to limit the depth of the structures to 10 or 12 feet; hence, the static soil stresses were in the range of 10 psi or less. To remain well within the larger limiting ground range indicated above, it was decided that the most distant structure location should be at a radius where the surface overpressure was expected to be approximately 100 psi. To remain conservatively within the overpressure radius of interest, it was decided that the closest structure should be at a ground range where approximately 300-psi surface overpressure was expected.

Chapter 2

PROCEDURE

2.1 DESIGN OF STRUCTURE

Two test structures and one comparison structure were used (Figure 2.1). Each test structure was a combination of an inner steel cylinder surrounded by a concrete pipe (Figure 2.2). The steel cylinder was approximately 2½ feet in diameter by 8 feet long and included a concrete slab bottom to provide adequate mass. This cylinder was enclosed by a reinforced-concrete pipe approximately 3 feet in outside diameter, 10 feet long, and open at both ends (Figure 2.3). The steel cylinder was separated from the concrete pipe by a shear barrier consisting of one rubber O-ring near the top and two O-rings near the bottom of the steel cylinder. The comparison structure consisted of the concrete pipe only. This pipe was identical to those used in the test structures, except that it had a concrete slab bottom. All these structures were placed with axis vertical and with the top approximately 2 feet below ground level (Figure 2.4). The test structures (but not the comparison structure) included a layer of frangible backfill (Figures 2.5 through 2.10) immediately outside the concrete pipe and below the bottom.

An octagonal concrete slab 15 feet across flats and 1 foot thick was placed flush with the ground surface above each of the structures (Figure 2.11). Each slab included a manhole and manhole cover and was designed to protect the structure against the direct application of overpressure (Figure 2.12). Figure 2.13 shows the assembly of the cylinders, concrete slab, and manhole cover in cross section.

One test structure and the comparison structure were placed at a ground range of 750 feet, where the overpressure was expected to be approximately 300 psi (Figure 2.14); the other test structure was placed at 1,050 feet, where the overpressure was expected to be approximately 100 psi. (As indicated in Figure 2.14, the actual pressures were 229 and 104 psi, respectively.) It was specified before the test that the precise overpressures to which these structures would be subjected were not critical to the experiment. The controlling principle was that they should be placed at the same radii at which measurements of the free-field earth phenomena were made by Projects 1.3 and 1.4 and be placed tangentially as close to these free-field measurement positions as was feasible.

The excavation for these structures was accomplished by power augering. For each structure a hole was augered 5½ feet in diameter and 15 feet deep. The backfill of dry sand was compacted by eccentric vibrators commonly used in the placement of concrete.

The project provided the test structures and the comparison structure, the shear barriers, and the frangible elements of the backfill. All the structures were prefabricated off-site.

The contractor at the site provided the holes and the concrete slabs complete with manhole covers and was responsible, under the supervision of project personnel, for placing the structures in the hole and backfilling.

2.2 DESIGN OF SPECIAL BACKFILL

As mentioned in Section 1.3, it was considered desirable that the frangible backfill should: (1) have small elastic compressive change of volume under the static overburden loads and

small plastic changes or creep under the static foundation loads; (2) be impervious to water; and (3) fail and form voids under the influence of stresses produced by explosions.

Consideration of various possibilities led to the conclusion that glass bottles were attractive from the standpoint of stiffness, water imperviousness, and good aging characteristics. It was further concluded that square shapes, with their better characteristics of fragility, would be more satisfactory than round ones. Specifically, it was recognized that the collapse under external pressure of square shapes was likely to be more uniform and at a lower value of pressure than that of round shapes.

As indicated earlier, it was desired that the frangible elements withstand, without failure, pressures of the order of 20 psi. It was desirable to find frangible elements that definitely would fail at pressures little above the value of 20 psi, since the project would fail to obtain data if the frangible backfill were not broken by the explosion forces.

Laboratory experiments on a wide range of sizes and shapes of glass bottles disclosed that square gin bottles most clearly fitted the desired specifications. Quart gin bottles were found to fail under external pressures ranging from 30 to 50 psi, with the major fraction falling between 35 and 45 psi. The next strongest alternatives tested were square milk bottles, which failed at pressures of approximately 65 psi. All bottles of smaller size withstood 100 psi successfully.

To avoid complete collapse, the bottles were placed around the side of the structure so that they covered about 53 percent of the area. Thus, there remained about 47 percent of the area in which the sand backfill was initially in contact with the structure (Figure 2.5). Since it was expected that the earth (motion) stresses and strains would be first a vertical compression and then a radial compression, it was decided that the bottles should be placed with their axes horizontal rather than vertical. With this orientation, the frangible backfill would be expected to collapse at an earlier time and under a lower total stress than with any other orientation.

The design of the frangible backfill below the bottom of the concrete pipe and of the inner cylinder required a very different approach, because the applied forces were expected to be of an entirely different character. It was estimated that the vertical motion of the soil at the 12-foot depth, where the bottoms of the structures were, would be a nearly instantaneous downward displacement of between 1 and 6 inches. If either, or both, the frangible backfill outside the concrete pipe and the rubber rollers between the inner cylinder and the concrete pipe served as satisfactory shear barriers, it was expected that the structures would remain essentially stationary during this downward displacement of the soil. Hence, the problem of designing the frangible backfill underneath the structures was primarily the problem of minimizing the upward acceleration required to reduce their velocity to zero at the time they returned to contact with the soil that had dropped out from under them.

Just as in the case of the frangible backfill at the sides, complete collapse of the bottom backfill was not desirable. For both the inner cylinder and the outer concrete pipe, the static vertical load was carried by the square bottles. To avoid the catastrophic collapse when the bottles broke, styrofoam columns were placed between the bottles. Preliminary tests showed that tapered columns (wedges) were superior to straight-sided ones; hence, tapered styrofoam columns were placed between the bottles under the inner cylinder, as shown in Figures 2.6 and 2.8. The weight of the outer cylinder (4,800 pounds) required eight bottles for support under static conditions, and the remaining space was sufficient only for straight-sided styrofoam columns (Figures 2.7 and 2.9).

Field experiments commonly develop information in unexpected areas, and it is only a penchant for complete recording which leads to reporting the following two items.

First, it was learned that all brands of gin do not come in square bottles, and an appropriate brand as acknowledged in the Preface was chosen after an extensive but not exhaustive test program.

A succession of raised eyebrows occurred during the routing of the requisition and order for thirty cases of gin bottles. In succession, all of the possessors of said raised eyebrows were finally convinced of the serious nature of the requirement, and with the blessing of the Bureau of Internal Revenue, the 30 cases finally arrived.

Second, the project requirement for 30 cases of empty bottles was a matter of surprisingly wide interest and there was a practically universal offer of assistance in all aspects of the procurement. The cooperative spirit displayed is gratefully acknowledged, and it is presumed that this spirit was shared by all other projects with equal enthusiasm.

2.3 INSTRUMENTATION

Dynamic recording instrumentation was limited to eight channels of acceleration as follows: (1) vertical and horizontal acceleration measured in the center of the bottom of the comparison structure, two channels; (2) vertical acceleration of the concrete pipe measured for each test structure, two channels; and (3) vertical and horizontal acceleration of the inner cylinder measured at the center of the bottom concrete slab for each test structure, four channels.

Standard Wiancko variable-reluctance accelerometers were used. Associated central equipment included 3-kc oscillators supplying carrier power to the transducers and to modified Wiancko demodulators. The demodulated signal was fed to oscillograph recorders.

In addition to the dynamic recording, measurements were made of the permanent displacement, both horizontal and vertical, of each structure. The measurement of the movement of one point on each of the concrete slabs was a responsibility of Holmes and Narver, Inc. Measurement of the permanent displacement of each of the underground structures relative to this point on the slab was the responsibility of Project 3.5.

Backup instruments were provided in the form of scratch gages and cork-and-string gages (Figure 2.15) as follows: (1) scratch gages to indicate relative motion, both vertical and horizontal (radial from ground zero), of the concrete outer cylinder of each of the three structures with respect to the slab at the surface; (2) scratch gages to indicate relative vertical motion only, between the inner and outer cylinders of the two test structures; and (3) cork-and-string gages to indicate maximum excursion and permanent displacement in the vertical direction of each cylinder with respect to the slab above it and of the inner cylinder with respect to the outer cylinder of the test structure.

2.4 EXCAVATION

In the spring of 1960 it seemed clear that there was an extremely low probability of further large aboveground explosions in Frenchman Flat, and hence, discussions were reinitiated leading toward the excavation of the structures to determine by observation exactly the state of the frangible backfill. It was planned to accomplish this work sometime during the fall of 1960, with the precise time schedule to be greatly influenced by other commitments of Stanford Research Institute (SRI) for work at the Nevada Test Site (NTS). Plans for the excavation were made and delayed by what proved to be false starts for further explosion tests.

Finally, in the early part of November 1960, the $\frac{1}{4}$ -inch steel plate cylinder shown in Figure 2.12 was torch-cut to separate it from the slab, and the slabs on the two test structures were then carefully removed by a crane. Care was taken not to disturb the structures and the backfill.

The schedule was again delayed by press of other activities; consequently, the structures were left open to the weather between November 1960 and 24 April 1961, when excavation actually commenced. In the meantime, a berm had been placed around each structure to prevent rainwater from filling the structures. This berm was effective at Structure 3 but was grossly ineffective at Structure 1 (Figure 2.14). Before excavation

commenced in April, it was necessary to dewater this structure.

Structure 3 was excavated completely before excavation was begun for Structure 1. The plan for each structure was to use a backhoe to dig an annular hole whose inner radius was approximately 1 foot outside the original augered hole. After this annular hole had been depressed to a depth of about 5 feet, project personnel excavated by hand the central mound so that the bottles were exposed. The annular hole was then deepened by the backhoe and this process repeated. Three lifts were required to reach the bottom of the structure.

Both to allow the excavation of the special backfill under the bottom of these structures in an undisturbed state and also to insure the safety of the people doing the excavating, it was necessary to support the structures during the latter part of the excavation. For this purpose, in the interval between the second and third deepening of the annulus, a 60-foot beam (56-foot clear span) consisting of two telephone poles lashed together was placed on two cribs located along a diameter of the hole. The inner structure was first lifted by the crane and was attached to the outer structure making use of the construction bolts provided for its transportation prior to original placement. The combined structure was then supported by a steel cable that passed between the two parts of the beam and over a hydraulic jack supported by them (Figure 2.16). The jack was operated to bend the beam to a deflection that had been determined by prior calibration to require a load slightly greater than the total weight of the structure. The whole procedure was successful, inasmuch as the structure lifted about $\frac{1}{4}$ inch as the excavation reached the bottom.

On Structure 3, as the excavation proceeded, the bottles were numbered in grease pencil as they were exposed. These numbers were in the form, b/r, where b is the bottle number with numbers 1 and 10 next to ground zero and the numbers running clockwise (as viewed from above), and r is the row number with Row 1 at the top and Row 30 at the bottom. The condition of each bottle (intact, cracked, or broken) was recorded as each row was uncovered. At intervals of five or six rows, photographs were taken of the bottles, one photograph of each quadrant. It was found as the excavation proceeded that the attachment of the bottles to the structure sides was insufficient to hold them in place for more than five or six rows, and hence, there was the danger that the bottles remaining on the structure would fall on the individuals performing the excavation as more and more rows were exposed. To make the operation safe, it was then decided to remove the bottles from the structure from time to time as the excavation proceeded. Thus, it was not possible to photograph the structure with all bottles attached, and composite photographs were prepared as Figures 3.12 and 3.13.

When Structure 1 was excavated, it was found that, after the first few rows, the bottles were so severely fractured that no numbering system was possible, and it was also found that the entry of water and silt had somewhat cemented sand and bottles to the structure. After the experience with Structure 3 (of having the excavated bottles and sand crumble at unexpected moments), long rubber bands were used on Structure 1, in an attempt to hold the excavated bottles and sand in place long enough to permit good photography. These bands, which show clearly in Figures 2.17 and 3.19, were useful but were not adequate to prevent more crumbling than would have been desirable from the standpoint of best photographic coverage.

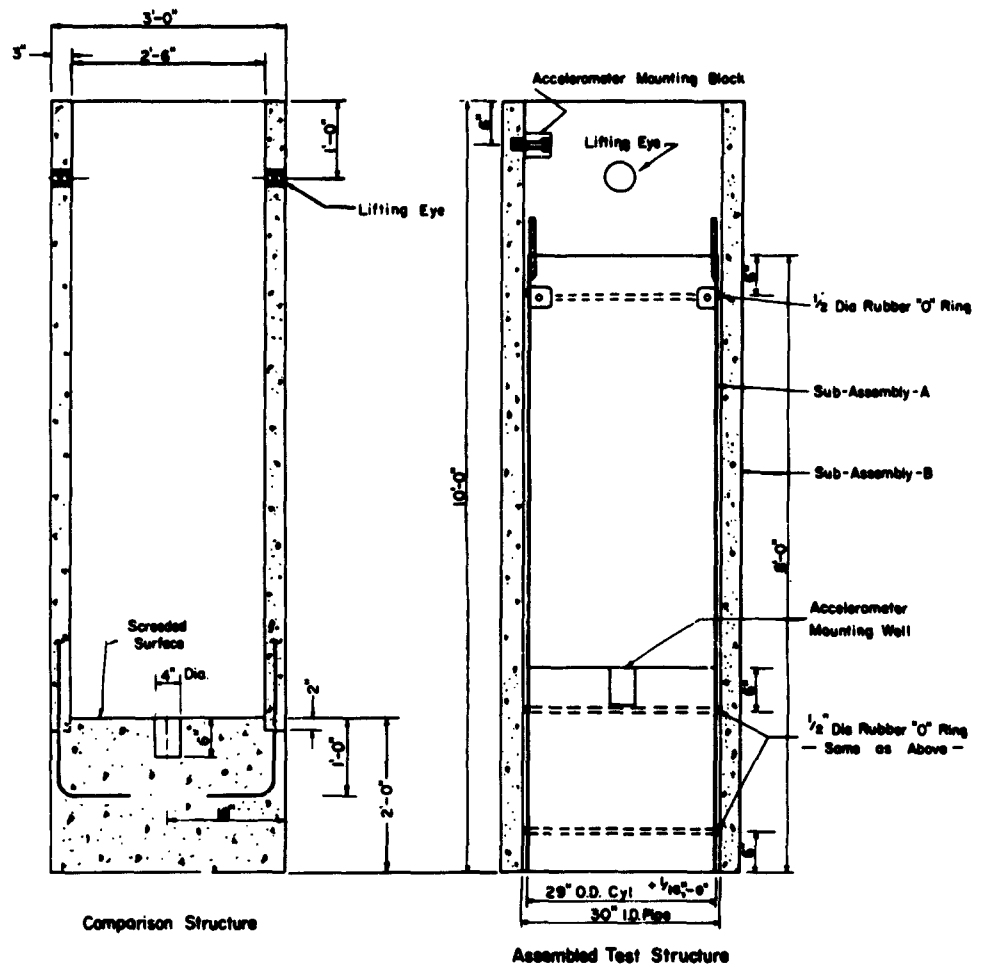


Figure 2.1 Comparison structure and test structure.

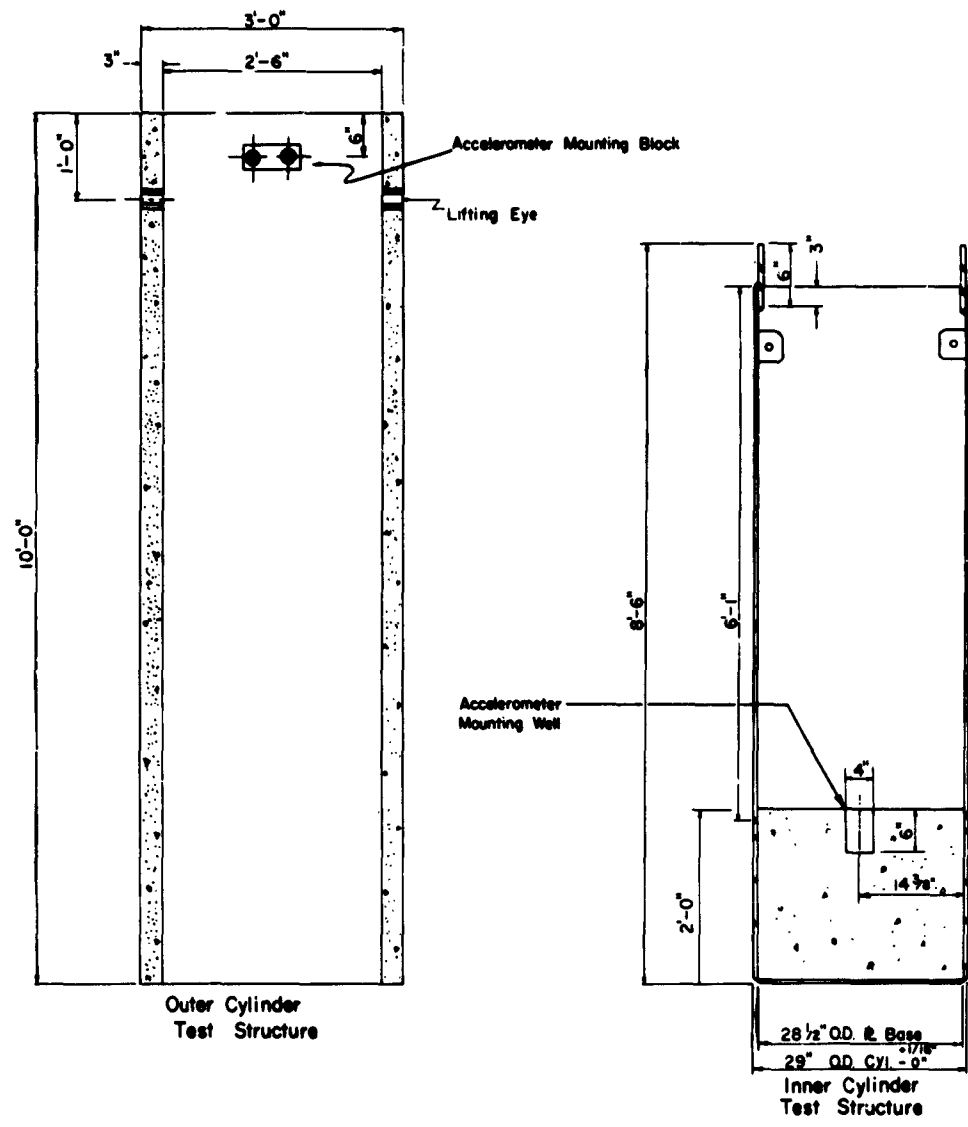


Figure 2.2 Cross section of inner and outer cylinders, test structures.

Figure 2.3 Reinforced concrete pipe, outer cylinder.



Figure 2.5 Frangible elements around outer cylinder of test structure.



Figure 2.4 Test structure and frangible elements in place in hole.



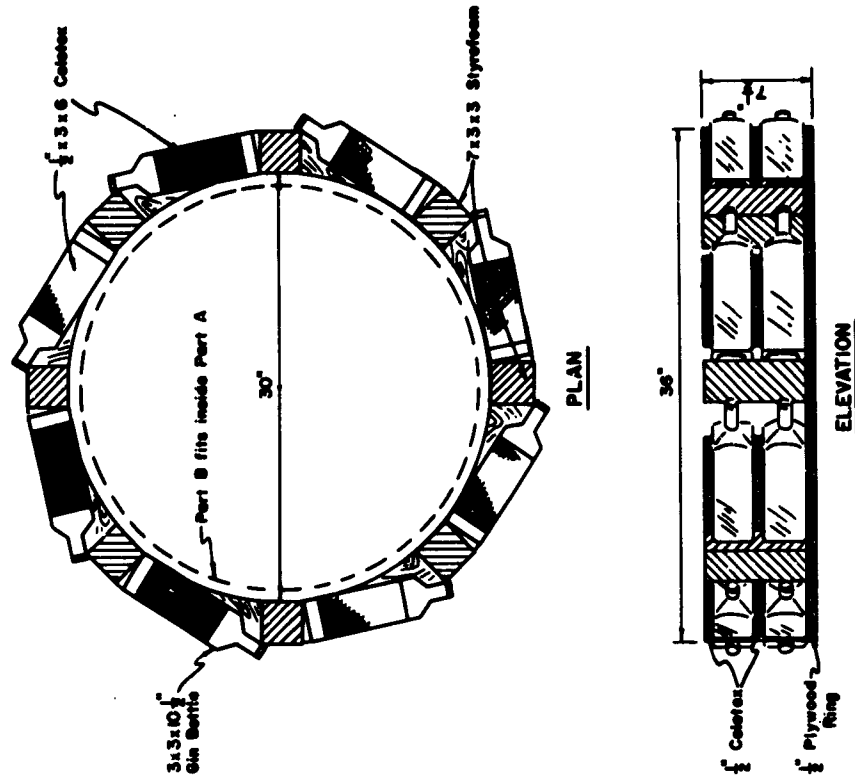


Figure 2.7 Plan and elevation views of base for outer cylinder.

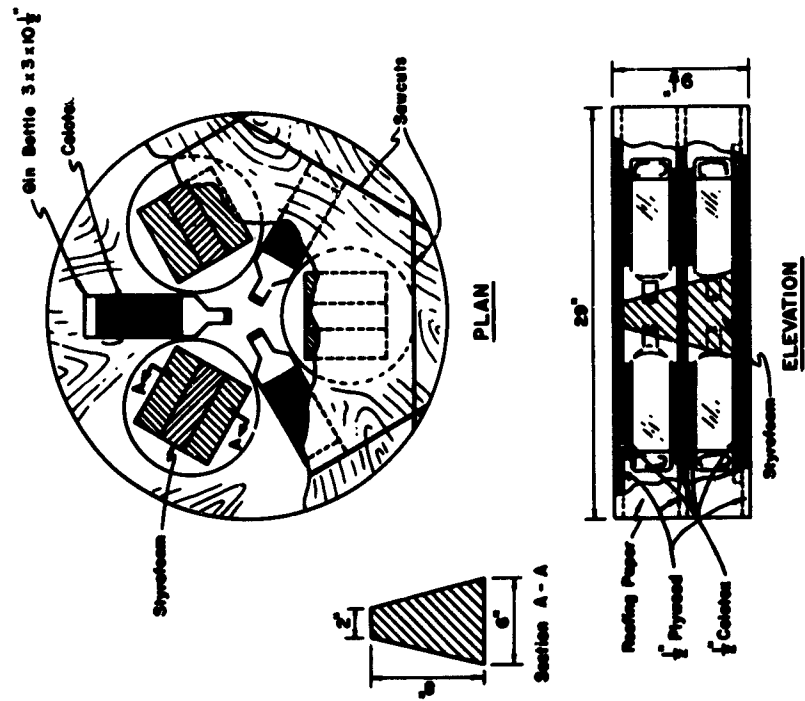


Figure 2.6 Plan and elevation views of base for inner cylinder.

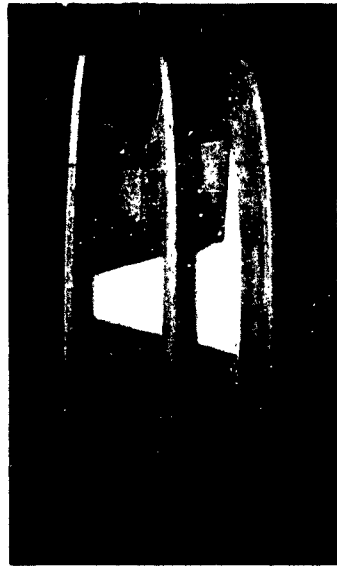


Figure 2.8 Inner cylinder base.

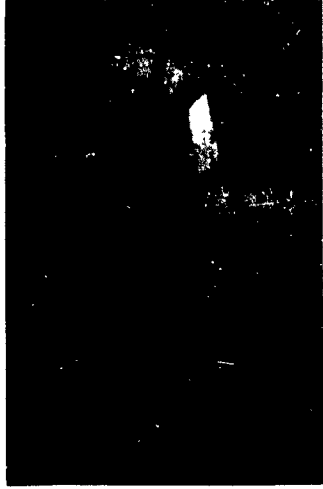


Figure 2.9 Outer cylinder base.

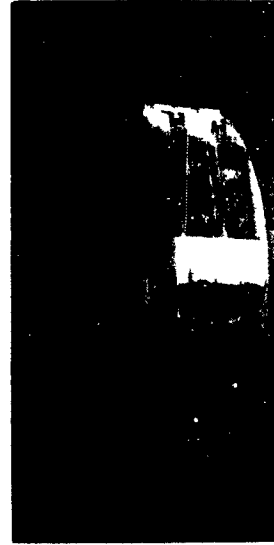


Figure 2.10 Bases for inner and outer cylinders, assembled.



Figure 2.11 Concrete slab and hatch cover.

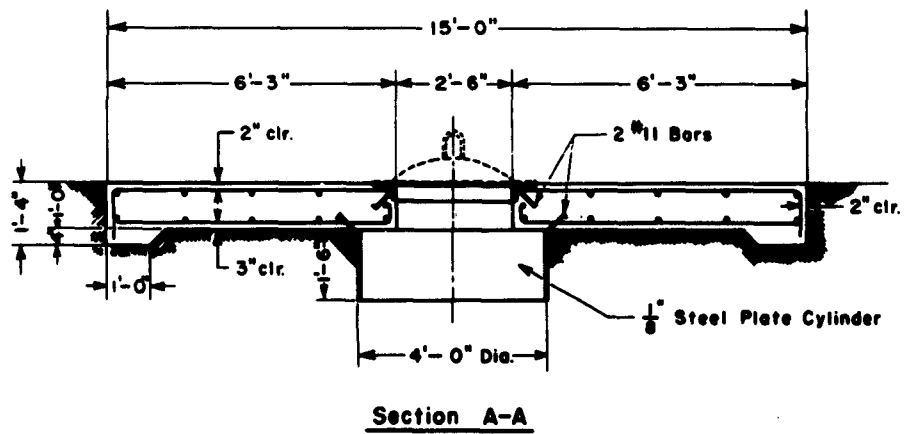
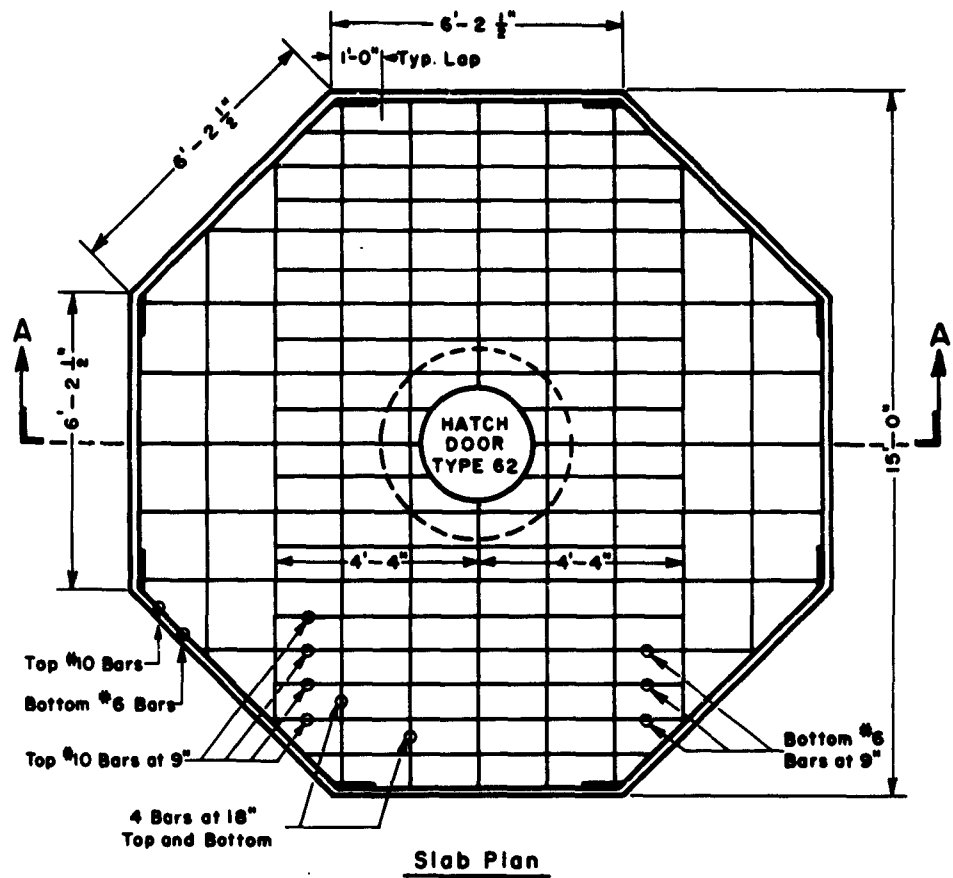


Figure 2.12 Details of concrete slab and hatch cover.

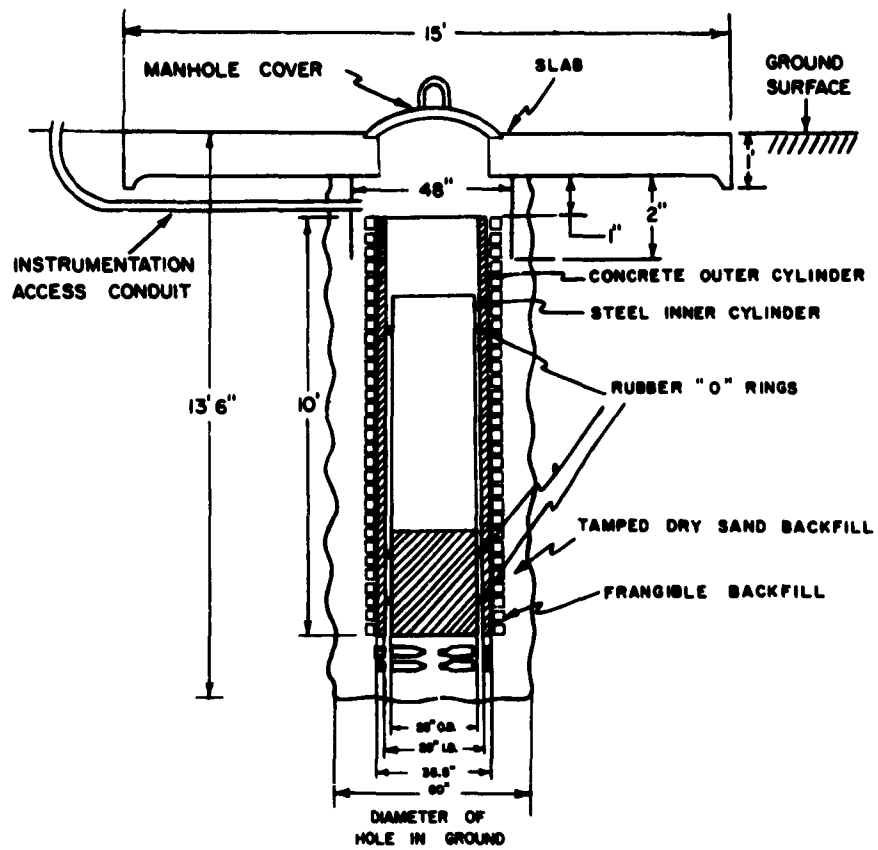


Figure 2.13 Cross section of test structure in place.

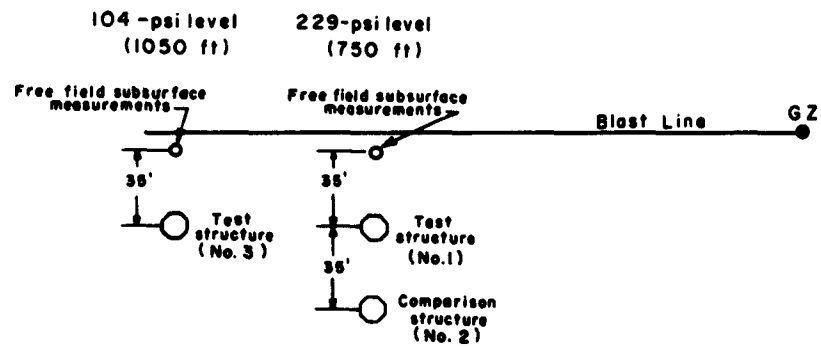


Figure 2.14 Structure locations.



Figure 2.15 Interior, Structure 3, showing scratch gages and cork-and-string gages.

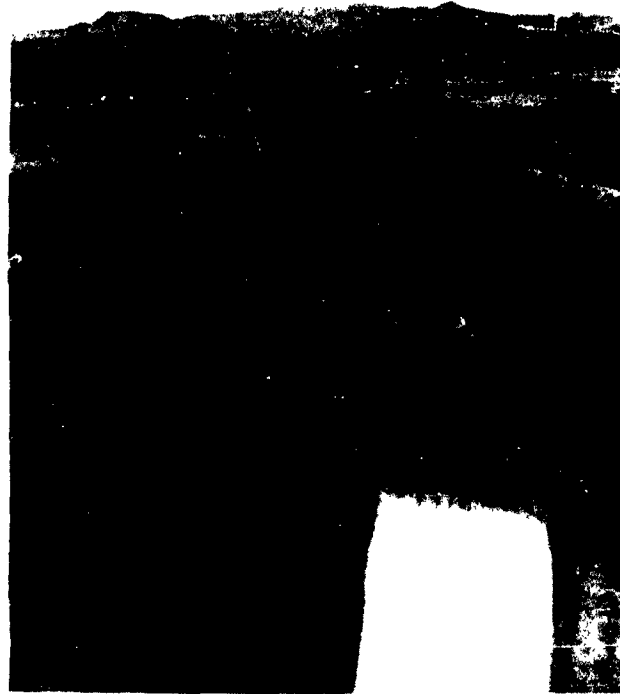


Figure 2.16 Support scheme for structure during excavation, Structure 3.



Figure 2.17 Excavating party at work, Structure 1.

Chapter 3

RESULTS AND DISCUSSION

The results of the experiment are summarized in Table 3.1, in which the peak values of structure motion are compared with the peak values of free-field motion.

3.1 ACCELERATION

The most significant result of the experiment was the reduction of the peak value of downward vertical acceleration. From Table 3.1 it is apparent that the frangible elements (bottles) at the sides of the structure, together with the sand backfill, reduced the peak downward acceleration of the structures to approximately 25 percent of that of the free-field earth acceleration at the same depths and distances. The rubber O-ring isolation of the inner cylinder produced a further improvement by a factor of approximately 5.

The peak upward acceleration of both the outer and inner cylinders at a ground range of 750 feet, amounting to some 5 or 6 g, was the acceleration experienced by the structure when it landed on the bottom backfill after the bottom of the hole had been suddenly displaced downward below the structure. While even these values amounted to reductions of more than a factor of 2 below the free-field values, they should be considered representative merely of this specific experiment and not of reductions that could be obtained by more extensive consideration of the design of the bottom backfill.

In regard to the figures for horizontal motion indicated by Table 3.1, it should first be noted that the Structure 2 moved with essentially the same peak acceleration and velocity as the free-field values, whereas the test structure at the same location, Structure 1 (the inner cylinder of which was protected by both frangible backfill and rubber O-rings), sustained horizontal accelerations only 15 percent of those sustained by either the free-field or the comparison structure.

A more detailed presentation of the results of the experiment is contained in Figures 3.1 through 3.6, which show the time curves of acceleration, velocity, and displacement of the structures and the soil at the same radii and depth. In these graphs, upward quantities are plotted as positive.

In the upper graph of Figure 3.1, the surface overpressure and the free-field vertical acceleration of the soil at depths of 1, 5, and 10 feet are shown together. The great reduction in the peak acceleration as the wave traveled downward through the soil as well as the change in character of the acceleration curve is apparent on this graph. In the center plot of Figure 3.1, the free-field vertical acceleration at 10-foot depth is plotted again but to an expanded scale, and the vertical accelerations of both the outer and the inner cylinders of Structure 1 are shown for comparison. The difference between the vertical acceleration of the outer structure as shown on this curve and the free-field acceleration at the 10-foot depth clearly illustrates the benefit of the frangible backfill and sand. Similarly, the difference between the vertical acceleration of the outer structure and that of the inner structure (dotted line) illustrates the beneficial effect of the rubber O-rings. As mentioned earlier, the 5-g upward peak acceleration of the inner structure, which occurred at 0.325 second, was the acceleration the structure experienced upon landing on the support provided for it at the bottom of the hole. It is believed that this peak could be reduced to any desired value by giving more attention to the

bottom support. In fact, it is suspected that there was a slight misalignment as the structure was placed on the support in the hole so that one edge of the inner structure landed on a part of the support provided for the outer cylinder. Because of the greater weight and smaller area of the annulus of the outer structure, the bearing load for it was several times greater than that for the inner structure. As a result, the support was necessarily stiffer; and if the inner structure landed partly on the stiff support provided for the outer structure, a relatively high acceleration would be expected.

The experiment design included measurement of vertical acceleration of the comparison structure, and incontrovertible evidence of the effect of the special backfill would have been provided by comparison of the vertical acceleration of the comparison structure with that of the test structure at the same radius. Unfortunately, one of the few instrumentation losses for this project was that of the vertical acceleration of the comparison structure. The lower plot of Figure 3.1 shows the similarity of the horizontal acceleration of the comparison structure and the soil at 10-foot depth and the gross difference of these values with the acceleration of the inner cylinder of the test structure. The similarity of the horizontal acceleration of the comparison structure with that of the free field at 10-foot depth is the best evidence available that the comparison structure did in fact move essentially like the soil at the 10-foot depth. It is largely on this basis that the authors of this project rest the validity of the comparison of the vertical acceleration of the soil at 10-foot depth. The inner test structure was protected against horizontal acceleration both by the rubber O-rings that separated it from the outer cylinder and also by the bottles and sand that separated the outer cylinder from the soil. Thus, a comparison of the dotted curve on the bottom graph of Figure 3.1 with either the comparison structure or the free field represents the benefit obtained by the combination of the frangible backfill and the rubber O-rings.

In the 104-psi surface overpressure region, the benefit of the frangible backfill would have been best illustrated by comparing the vertical acceleration of the outer structure with that of the free field at 10-foot depth. Since this free-field measurement was not made, it is necessary to estimate that the curve for this depth lay between that for 5 feet and 20 feet, as shown in Figure 3.2.

The lower graph of Figure 3.2 permits comparison of the horizontal acceleration of the inner test structure at this radius with the free-field horizontal acceleration at 10-foot depth. It is to be remembered that this shows the combined benefit of the rubber O-rings, together with the bottles and sand.

3.2 VELOCITY

All the acceleration-time oscillograms were transformed to digital form on IBM cards and were integrated to obtain velocity versus time curves. Trial plots of these velocity curves were made, and an adjustment of each one was made arbitrarily to bring the velocity to zero at a reasonable time. This adjustment amounted to a shift of the zero line for the accelerometer. The magnitude of the adjustment was almost always small, usually little more than the thickness of the line on the acceleration plot. These adjusted velocity curves are shown in Figures 3.3 and 3.4. On these graphs the symbol ⊕ indicates the unadjusted value of the velocity at the time when the velocity was adjusted to be zero.

In general, the velocity correction was made as far out on the time scale as the report authors felt the individual curve to be reliable. This means that when the curve was plotted beyond the point of correction, it was done to squeeze the last vestige of value out of the data and with an awareness that the resulting curves might be misleading. To indicate the uncertainty, all velocity curves carried beyond the correction point were dashed if they were previously solid and had dots inserted if they were previously dashed.

Evidence collected as part of Project 1.4 (Reference 1) indicated that the wave front

of the major compression wave in the soil at the 200-psi level was inclined at 9° to the horizontal and at the 100-psi level at 11° to the horizontal. This means that the main particle motion was nearly vertical and, hence, that the frangible backfill was tested for the most part as a shear barrier rather than a compression barrier.

On Figure 3.3 it should be noted that the striking similarity in the surface overpressure waveform and the vertical velocity waveform at 1-foot depth is typical of kiloton tests.

The only suggested explanation for the fact that, in the bottom graph of Figure 3.3, the horizontal velocity of the comparison structure is larger than that of the soil at 10-foot depth is the possibility that the soil-sand-structure complex may have had a resonant frequency in the neighborhood of the frequency of the applied impulsive force. The records were carefully checked, and no instrumental or analytical errors were found.

In Figure 3.4, the striking similarity of waveform between the surface overpressure and the vertical velocity is again apparent. In the lower graph of Figure 3.4, the sinusoidal aspect of the structure velocity at about 0.4 second probably indicates a resonance determined essentially by the mass of the inner structure and the resilience of the O-rings. It should be noted that the magnitude of these velocities is small and is in fact trivial compared with either the vertical velocity at that radius or with the horizontal velocities of the structures nearer the burst.

3.3 DISPLACEMENT

The corrected or adjusted velocity curves described above were integrated once more to obtain displacement versus time curves (Figures 3.5 and 3.6). The process of double integration is fraught with unavoidable uncertainty, and it should be recognized that the displacements determined in this fashion are relatively unreliable and become progressively more uncertain at longer times after burst.

As is discussed further in a later paragraph, all the acceleration curves were artificially modified so that the velocities obtained by integration reached zero at a time arbitrarily chosen. In the 1-foot free-field record and the records of the structure, it was possible to make a more sophisticated judgment about the correction, because additional information was available in the form of scratch gage records. For this reason, on the middle graph of Figure 3.5 the curves for the 1-foot free-field and the structure displacement have been carried out to much larger times than the curves for displacements at 5-foot and 10-foot depths.

Since the corrections to the velocity curves were made to bring the velocity arbitrarily to zero at the time of the correction, the corresponding displacements obtained by integration at the time of the velocity correction were maximum values. In general, displacements shown after the time of velocity correction are considered unreliable and should be viewed in that light. In fact, in Reference 1, the report of the project covering free-field soil measurements, these displacement curves are not plotted past the maximum values. It is also to be noted that the vertical displacements at 1-foot depth reported here and in Reference 1 are not identical. This is because in Reference 1 the correction of the velocity was made for this gage on the same basis as for all other gages. In the present report, however, the velocity correction for this gage was modified to force the displacement to match somewhat better the scratch gage data described later.

On the middle graph of Figure 3.5 it is clear that the difference between the displacements at 1-foot and at 10-foot depths has a maximum of about 0.225 foot, or more than 2½ inches. This relative displacement over a distance of 9 feet amounts to an average strain of some 2.5 percent. It is of interest to note that while the soil at 10-foot depth was moving downward 2 inches, the outer structure moved downward only 1 inch and thereafter maintained rather small relative motion with respect to the soil. Thus, there was more than 1-inch shear strain between the outer structure and the soil at any point around its sides. Similarly, the inner structure moved even less than the outer. The

maximum relative displacement between these two was of the order of 3 inches. It should also be noted that the displacement curve for 1- and 5-foot depths as shown on the graph indicates that the movement at 5-foot depth was ultimately greater than that at the 1-foot depth. On general grounds it is judged to be quite certain that the movement at 5 feet was less than that at 1 foot. The contradictory indication of the curves simply demonstrates that there are important cumulative errors inherent in any process of double integration. In fact, returning to Figure 3.3 and noting the corrections applied to 4V1 and 4V5, it is found that the corrections to these two curves, which were made at about 0.355 second, total some 5- or 6-ft/sec for each curve. The corresponding correction in the displacement figures at this time is about 1.5 feet for each curve. Thus, if the uncorrected velocity curves had been integrated, the displacements shown would be some 3 feet different from those actually shown, and the 1-foot record would show a greater displacement at all times than the 5-foot record. This means simply that the corrections actually applied to the velocity curves were in these two cases probably somewhat larger than they should have been.

The bottom graph of Figure 3.5 permits comparison of the horizontal displacements of the comparison structure, test structure, and 10-foot free-field depth. It will be noted that the comparison structure apparently moved considerably more than the free field. This was a surprising result and led to a meticulous review to be sure no instrumental or computational error had occurred. The accelerometers from which these displacements were derived were identical Wiancko gages both with 30-g rated values (and hence registering above 30 percent of rating as shown on the bottom graph of Figure 3.1) and with natural frequencies of 85 cps. These gages were connected to identical galvanometers having natural frequencies of about 300 cps. Thus, a careful check of the instrumentation and the data reduction confirmed the validity of the curves.

The only explanation suggested was that the comparison structure was some 70 feet in a tangential direction away from the free-field gage, and since the whole experiment was in a precursor region, it was possible that the airblast input was significantly different at the location of the comparison structure than it was at the free-field gage. There was, of course, a significant difference in the properties of the structure from those of the surrounding soil with the structure both considerably stiffer and more dense than the soil. These differences might have explained some delay in the motion of the structure behind that of the soil but did not satisfactorily explain the greater displacement.

Figure 3.6 displays the displacement of the test structure and the free field in the 104-psi region. The same remarks apply to this figure as to the curves of Figure 3.5 regarding uncertainty of the displacement curves after the peak values. It is also true that the 6V1 velocity was corrected to force the displacement to fit scratch gage data at early times. The implication in the middle graph of Figure 3.6 that the displacement at later times for 1-foot depth is less than that for 5 or 20 feet is not believed to be true. It indicates rather the gross uncertainty of displacements at later times when they are obtained by double integration of accelerometer records.

In the bottom graph of Figure 3.6 the horizontal displacement of the inner test structure is compared with the 10-foot free-field displacement. The oscillation of the inner structure is presumed to be at the natural frequency determined by the mass of the inner structure and the resilience of the rubber O-rings separating it from the outer structure. It is to be noted that the displacement scale had to be expanded greatly to make these curves visible.

Figure 3.7 compares the relative motion of Structure 1 determined by the scratch gage (Figure 2.15) with that determined by computational subtraction of the appropriate displacement curves obtained by double integration of accelerations. The displacement scale on Figure 3.7 is full scale. Thus, referring to the right-hand figure, the scratch gage record shows that the slab moved with respect to the outer cylinder a downward distance of nearly 5 inches, moved upward to a height nearly 4 inches above its initial

position, returned to a position close to the start, and went through another complete cycle, finishing at a point about 1 inch lower than the start. The correspondence shown in the left-hand figure with the initial motion as indicated by the scratch gage is somewhat artificial, since the 4V1 record was adjusted partly on the basis that this correspondence was appropriate. The comparison suggests that there was extensive relative motion later than 800 msec after shot time. It might, perhaps, have been more appropriate to have made the 4V1 adjustment so that the downward relative displacement indicated by numerical difference was somewhat smaller than that indicated by the scratch gage, because it is probable that the center part of the slab moved downward more than the 1-foot free-field gage. The slab was, in fact, supported largely near the outer edge, and the center could have deflected as much as 1 inch more than the 1-foot free-field value. About $\frac{1}{2}$ inch might have been due to elastic bending in the slab and the other $\frac{1}{2}$ inch to compression of the soil near the rim because of the higher pressure of the slab against the soil.

Figure 3.8 displays a similar comparison of the scratch gage record showing the relative motion of the outer and inner cylinders of Structure 1 with corresponding relative motion determined by subtraction of integrated accelerometer readings, in the same fashion as was used for Figure 3.7. The accelerometer records were adjusted during integration to force approximate agreement in peak measurement of the downward motion. As the figure shows, the record by accelerometer departs seriously from the scratch gage in the indicated upper displacement.

Figure 3.9 is the scratch gage record of Structure 2. It shows the displacement of the slab relative to the structure. Since the vertical acceleration of this structure was lost, it is not possible to make a comparison corresponding to those of Figures 3.7 and 3.8.

In Figure 3.10, the scratch gage record of Structure 3 is compared with the displacement determined by acceleration. In the same manner as with the other comparisons, adjustment was made of the acceleration, and as the figure shows, the correspondence was somewhat less than satisfactory. In fact, it shows in graphic fashion the significant uncertainty in displacement determined by double integration of accelerations.

The nonelectronic methods of backup measurement were of three types: (1) direct measurement or survey, (2) scratch gage, and (3) cork-and-string gage.

The relative horizontal permanent displacement of each structure with respect to the slab above it is given in Table 3.2. Since no electronic measurements of the slab motion were made, it is not possible to compare permanent relative horizontal displacement obtained by integrating accelerations with the values obtained by direct measurement. The figures in Table 3.2 seem entirely reasonable and are not inconsistent with any other observations. They show that the structures did not tilt appreciably. The only mildly surprising result was the indication that Structure 3 sustained a permanent displacement away from ground zero (relative to the slab).

A line of levels was run by Holmes and Narver, Inc., before and after the shot. The permanent vertical displacements of the slabs determined by those measurements are collected in Table 3.3. The difference in motion shown between the slab above Structure 1 and that above Structure 2 supports the suggestion that there was some azimuthal dissymmetry in the blast wave. The two slabs were identical, and the holes for the structures were identical; therefore, it would be expected that the slab displacements would be identical.

The results of the scratch gage measurements and the cork-and-string gage measurements are collected in Table 3.4. In general, these two measurements were gratifyingly consistent and were felt to be quite reliable. No comparison is made here between the maximum relative displacement obtained by scratch gage and that obtained by integrated accelerations, because, as noted earlier, the acceleration records were adjusted during the integrations to force a correspondence of the first peak values.

3.4 EXCAVATION

3.4.1 Structure 3. The results of excavating Structure 3 is illustrated by the schematic diagram of Figure 3.11, which is a developed view of the bottles surrounding the sides of the structure. It can be seen from the figure that 27 percent of the bottles were broken, that there was no significant azimuthal dissymmetry, and that there was considerably more damage in the top half than in the bottom half. Actually, it is suspected that the broken bottles in the lower rows were probably broken during placement, inasmuch as the dry sand was vibrated in place with eccentric vibrators used for concrete placement, and it was difficult for a workman to control the position of the vibrator, particularly in the deeper parts of the hole. The photographic evidence equivalent to Figure 3.11 is displayed in Figures 3.12 and 3.13.

As the excavation of this structure proceeded to the bottom, the structure, now supported by cabling attached to beams across the top of the hole, lifted about $\frac{1}{4}$ inch and swung about $2\frac{1}{2}$ inches laterally from its position in the soil (Figure 3.14). Of the two rows of eight bottles each, which supported the outer test structure, all were cracked except two in the top row and one in the bottom row. These three intact bottles were all in the direction of ground zero. Figure 3.15 illustrates that, although the remainder were cracked, they were not seriously crushed. The fact that they were not crushed confirms broadly the curves of Figure 3.6, which indicate that the soil at depths of 5 feet and 20 feet moved downward some 0.2 or 0.3 foot farther than the outer test structure. The fact that they are cracked implies that, in the early stages of the explosion wave, there was a slight relative motion of compression between the soil at the bottom of the hole and the structure. This does not show on the time records of displacement determined from double integration of acceleration measurements. It is, however, within the range of uncertainty of those data.

The inner base (Figure 3.16) had all three top row bottles broken and all three bottom row bottles unbroken. Since the differences in force on these two rows can only occur as the result of inertial forces on the bottles themselves, the implications of breakage of one row and not the other are unclear. The fact that the bottles were not crushed confirms still further the record in Figure 3.6 showing that the structure and the earth below it parted company and did not come together again.

The concrete slab over the structure had the function of preventing air-pressure forces from entering the interior of the structure. For this purpose the slab redistributes the air pressure applied to its top surface directly above the hole and transmits to the soil a somewhat increased pressure over the annulus. Since the area of the central part is only about 5 percent of the total slab area, the increase in pressure applied to the soil is only about 5 percent. This anomaly in soil pressure will die away with depth and can account for a small increase in stress applied to the bottles around the top half of the structure. The air overpressure curves show a reasonable approximation to the classical sharp rise and exponential decay, but it can be noted that for Structure 1 the air pressure is close to 200 psi for an interval of more than 10 msec and above 175 psi for about 20 msec (Figure 3.5). In the case of Structure 3, the pressure is above 80 psi for about 40 msec (Figure 3.4). The wave velocity for stresses of this magnitude in Frenchman Flat near-surface soil is about 700 ft/sec so that 10 msec corresponds to 7 feet, and 40 msec to 30 feet. This means that it is a reasonable approximation to consider that the structures were subjected to steady-state stresses of the magnitude indicated, even though the actual problem is of course a dynamic one. Consideration of natural period of component elements of the structure leads to the same conclusion, in that all the natural periods are small compared with 10 msec, except perhaps the horizontal linear mode of the combination of the inner structure, rubber O-ring, and outer structure. A glance at Figure 3.4 suggests that the period of this oscillatory system lies between 40 and 80 msec.

The static external air pressure tests on the bottles showed their failure at approximately 40 psi. It is inferred from the results on Structure 3 that the peak stress on the bottles around the upper half exceeded 40 psi. In both cases it seems clear that the radial strains were quite small, since even the broken bottles were not filled.

3.4.2 Structure 1. The excavation of Structure 1 was begun on the same basis as used on Structure 3. The first two rows of bottles, which were fully protected by the $\frac{1}{8}$ -inch steel cylinder attached to the slab are shown in the top photograph in Figure 3.17. The numbering system used previously was also inaugurated here but was abandoned after Row 4 because of the conditions shown in the lower photograph in Figure 3.17. These photographs and those in Figure 3.18 show the complete breakage and crushing, which ultimately was found for all the rows below Row 3. There was, in fact, no azimuthal dissymmetry and almost no depth dissymmetry. All the bottles were completely broken and crushed in such fashion that the envelope of their outer surface appeared to be moved in about 2 inches on the radius. This implies that all the voids provided by the bottles were completely filled. The only minor exception to the complete breakage and crushing occurred in the lower three rows of bottles as illustrated in Figure 3.19 where it can be seen that, although the bottles are cracked, they are not totally crushed and are not fully filled with sand.

When the bottom of this structure was reached, it was clear that the structure had been placed slightly off-center on the frangible subbase during its original positioning. This offset amounted to about 2 inches (Figure 3.20). The lower photograph in this figure also shows the extent of flooding incurred between November to April while the structures were left open; it also shows the trace of the rubber O-ring seen in the upper photograph in Figure 3.21. It is clear from these pictures that the flood waters washed the O-ring down from its installed position, about 18 inches higher, so that one part of the O-ring finally entered the open space beneath the structure, as shown in the lower photograph in Figure 3.21. In the outer subbase, there were only three unbroken bottles, one in the top row and two in the bottom row. All these were in the general direction of ground zero. The broken bottles were noted to be full of silt rather than sand. It is clear from the lower photograph in Figure 3.21 that this structure, like Structure 3, parted company with the soil below it and never remade contact.

The inner subbase, as shown in Figure 3.22, had two bottles in the top row and one bottle in the bottom row unbroken. One of the unbroken bottles in the top row was found to be one-quarter full of water. Since, in fact, the bottles had been received empty but capped and sealed, there was a minor mystery. It is presumed that, during the rainy season, this bottle had an external water pressure on it amounting to several feet of head and that the seal was not perfect. Then, since the bottle was on its side, as the water level receded below the bottle, the water that entered was trapped inside.

3.5 SOME THEORETICAL CONSIDERATIONS OF BOTTLE BREAKAGE

An attempt is made here to correlate the observed breakage of the bottles with some very simple theoretical considerations. Of necessity, many simplifying assumptions must be made. One of these assumptions is that the situation is treated statically instead of dynamically. This is reasonable, because the duration of the peak overpressure is long compared to the time for seismic waves to travel the dimension of the cylinder.

Two different approaches are taken here. First, the volume change occurring in an unsupported hole in an elastic half-space is considered in an attempt to correlate this volume change with the volume of the bottles that were found to be completely filled with sand. Second, a soil mechanics approach is taken, to estimate the horizontal stress on the bottles from some measured values of the vertical stress. These horizontal stresses are then related to the known crushing strength of the bottles. Further, the air pressure

on the ground surface necessary to cause failure of the unsupported hole is estimated.

3.5.1 Volume Change of Unsupported Elastic Hole. The ground is considered to be a simple elastic medium, and a comparison is sought between the volume change per foot depth of an unsupported hole and the volume per foot depth of the bottles that were found to be more or less completely crushed and filled with sand.

For this purpose a uniform elastic half-space is first assumed, which is subjected to the vertical pressure q over a circular area of radius a . Stress distribution in the volume underneath the circular area for this model has been determined on Page 366 of Reference 2; and from the stresses at the surface of an imaginary vertical cylinder underneath this circle, it is possible to determine the volume change within it. If a set of equal but opposite stresses are applied to this cylindrical surface, an additional volume change will be produced. Since the superposition of these two sets of stresses leaves the cylindrical surface free of stress, the enclosed cylinder is equivalent to a cavity. This method is suggested on Page 410 of Reference 3. The solution in detail is as follows.

First, consider a half-space subjected to a vertical pressure q over a circular area of radius a . Then from Reference 2 the radial compressive stress σ_r and circular compressive stress σ_θ for points not too far distant horizontally or vertically from the center of the overpressure circle are given by

$$\sigma_r = \sigma_\theta = \frac{q}{2} (1 + 2\nu) \quad (3.1)$$

Where: ν = Poisson's ratio.

The vertical compressive stress $\sigma_z = q$, and the shear stresses are small. Then, for a cylinder of radius r ($r < a$) and height h ($h < a$) subjected to these stresses, the change in volume is

$$\delta V_1 = \pi r^2 h \frac{(\sigma_r + \sigma_\theta + \sigma_z)}{3\lambda + 2\mu}$$

where λ and μ are Lamé's elastic constants. Therefore,

$$\delta V_1 = \pi r^2 h \frac{2q(1 + \nu)}{3\lambda + 2\mu} \quad (3.2)$$

Now imagine this stressed cylinder removed from the full half-space, leaving the cavity as desired. This is equivalent to adding tensile forces equal to σ_r over the cylindrical cavity. Regarding now the half-space with the hole in it as a thick shell of infinite external radius, it is possible to obtain further decrease in volume given by

$$\delta V_2 = \pi r^2 h \frac{\sigma_r}{\mu} = \pi r^2 h \frac{q(1 + 2\nu)}{2\mu} \quad (3.3)$$

Total volume change of the cavity is then

$$\begin{aligned} \delta V &= \delta V_1 + \delta V_2 = \pi r^2 h \left\{ \frac{q(1 + 2\nu)}{2\mu} + \frac{2q(1 + \nu)}{3\lambda + 2\mu} \right\} \\ &= \frac{\pi r^2 h q}{E} (1 + \nu) (3 - 2\nu) \end{aligned} \quad (3.4)$$

The hoop stress is now given by $\sigma_\theta = q(1 + 2\nu)$, that is, double that of the solid half-space.

The properties of the soil at Frenchman Flat have been measured many times, and the range of values is somewhat disturbing. Reasonable values appear to be (Reference 4)

$$\nu = 0.38$$

$$E = 7,000 \text{ to } 12,000 \text{ psi}$$

Then, for a 1-foot length of Structure 3, $r = 18$ inches, $h = 12$ inches, $q = 100$ psi, and $\delta V = 540$ to 310 in³ per foot of depth.

The total of 300 quart bottles amounts to $17,400$ in³, i. e., $1,740$ in³ per foot of depth, so that the two values of δV correspond to 31 and 18 percent, respectively, of the available volume in the bottles. Now in this test in Rows 5 through 10, roughly 75 percent of the bottles were broken and 30 percent of these were filled, and this is of the order of the ratio of the volume change of the hole to that of the volume of the bottles.

If the same analysis is applied to Structure 1 with an incident pressure of 229 psi, then the values of δV correspond to 71 and 41 percent, respectively, of the available volume. This model then does not fully account for the complete breakage and filling that occurred on Structure 1. This implies that either the modulus is lower than 7,000 psi or that the soil was stressed beyond its elastic limit. The latter is believed to be more plausible and is discussed in the next section.

3.5.2 Soil Mechanics Approach. Here the problem is divided into two phases: the initial or small deformation phase, and the failure or large deformation phase.

It is assumed that, during the first moments of loading, the deformation is essentially vertical, and the soil does not fail. In this case the horizontal stresses can be related to the vertical stresses induced in the soil. This relation is

$$\sigma_r = K_0 \sigma_z$$

Where σ_r = lateral or radial stress

σ_z = vertical stress

K_0 = an empirical constant called the coefficient of earth pressure at rest.

Immediately around the layer of bottles there is a 1-foot-thick backfill of well-compacted, dense, angular sand. In dense sand, K_0 ranges from 0.5 to 0.8, but in the silty clay surrounding the sand, K_0 is about $1/3$. Therefore, it is reasonable to choose $K_0 = 0.5$ for the present case.

In a static case, there would be essentially no variation of σ_r or σ_z over the depth of the structure. However, in the dynamic case, it is known that vertical stress attenuates with depth. The curves for σ_z in Figure 3.23 have the form of the variation with depth given in the test results of Reference 1. By applying the factor K_0 , values of σ_r were obtained and also depicted in the figure. Notice that σ_r for Structure 3 at the bottom is below the bottle strength, so that the bottles there would not be expected to break. Since the situation is actually dynamic and the direct overpressures are not the only forces acting, the horizontal stresses may be much different from those in the figure.

If the frangible backfill fails at the values of σ_r given above, the soil deforms and failure surfaces appear. In the usual soil mechanics approach, a region of plastic equilibrium is assumed, and the analysis proceeds to determine the extent of the region and the boundary forces required. It is no longer possible to assume that the sand and clay act together as a unit. So much motion may occur in the sand that there is little pressure between the sand and the clay surrounding it. Actually, the sand may lose contact with the concrete cap, thus reducing the vertical stress and the lateral resistance. Therefore, the clay may fail. In the following, the value of the overpressure P_0 necessary to cause failure around an unsupported hole in a rigid-plastic soil is determined (Figure 3.24). The normal assumptions of soil mechanics are made, i. e.,

- (1) Homogeneous soil.
- (2) Full strength utilized at all times.
- (3) Failure by rigid-plastic translation of the wedge and a conical failure surface.
- (4) Applicability of Coulomb's law, i. e., $s = C + \tan \phi$.

Where: s = shearing resistance on the slip plane per unit area

C = cohesion of the soil

σ = normal stress on the shearing plane

ϕ = angle of shearing resistance

(5) Negligible variation of the earth pressure on the sides of the wedge with depth.

(6) Cylindrical symmetry.

Figure 3.24 shows the geometry of the system. N and N_1 are the forces normal to the planes indicated, and W is the weight of the soil in the wedge. The shearing force on the plane of failure is given by S . Useful geometric properties of the wedge are

$$\text{Volume of the wedge} = \frac{h^2}{2} \cot \Theta \left(R + \frac{h}{3} \cot \Theta \right) \alpha$$

$$\text{Plane area of wedge} = A_p = \frac{h}{2} \cot \Theta (2R + h \cot \Theta) \alpha$$

$$\text{Failure plane area} = A_f = \frac{h}{2} \operatorname{cosec} \Theta (2R + h \cot \Theta) \alpha$$

When the soil is at failure, the shear stress on the failure plane is given by Coulomb's equation. The maximum overpressure that can be withstood before failure of the soil can be determined using the Coulomb failure criterion and the equations of equilibrium in the radial and vertical directions. These three equations are

$$N \sin \Theta - S \cos \Theta - N_1 \alpha = 0 \quad (\text{radial})$$

$$-N \cos \Theta - S \sin \Theta + P_o A_p + W = 0 \quad (\text{vertical})$$

$$S = C A_p + N \tan \Theta \quad (\text{Coulomb})$$

Approximations in these equations are that $\sin \frac{\alpha}{2} = \frac{\alpha}{2}$ and $\cos \frac{\alpha}{2} = 1$. The circumferential stresses are computed by multiplying the coefficient of earth pressure at rest, K_o , times the vertical stresses. Summing these over the vertical surfaces of the wedge results in $N_1 = \frac{K_o h^2}{2} \cot \Theta (P_o + \frac{\gamma h}{3})$. A simultaneous solution of the three equations for S , N , and P_o results in

$$P_o = \frac{C \left(2 \frac{R}{h} + \cot \Theta \right) \left[1 + \tan (\Theta - \phi) \tan \Theta \right] + \gamma \left[\frac{K_o h}{3} - \left(R + \frac{h}{3} \cot \Theta \right) \tan (\Theta - \phi) \right]}{\left(2 \frac{R}{h} + \cot \Theta \right) \tan (\Theta - \phi) - K_o}$$

The following values are taken from Reference 4.

$$C = 2,400 \text{ psf}$$

$$R = 2.75 \text{ feet}$$

$$h = 13.5 \text{ feet}$$

$$\phi = 30^\circ$$

$$\gamma = 88 \text{ pcf, the unit weight of the clay}$$

Assume $K_o = \frac{1}{3}$. Then at $\Theta = 65^\circ$, P_o has a minimum value of 123 psi. The actual overpressure q is applied to an octagonal concrete slab of area 186.3 ft^2 , which is unsupported over a central region of $\pi 2.75^2 = 23.8 \text{ ft}^2$. Therefore,

$$q = \frac{186.3 - 23.8}{186.3} 123 = 107 \text{ psi overpressure.}$$

Since the dynamic shear strength of this soil is certainly larger than the static strength (perhaps as much as double), it appears that the overpressure load that would have caved in an unsupported hole lies between the 104 psi applied to Structure 3 and the 229 psi applied to Structure 1. The observed damage to the bottles in both structures is thus consistent with this elementary analysis.

Since the bottles were broken about as predicted by the small deformation analysis of soil mechanics, it can be concluded that the soil did not fail before the destruction of the frangible backfill. When the frangible backfill is destroyed, subsidence occurs. For small overpressures, only the sand yields, but for large pressures the clay fails also. Equilibrium is regained with some small radial pressure. The elastic analysis concurs in this by demonstrating that the backfill behaved elastically at Structure 3 but yielded somewhat at Structure 1.

3.6 SUMMARY OF RESULTS

In summary, the results of the backup measurements show that:

1. The relative vertical movement between the slab and the two elements of Structure 1 amounted to total excursions in the range of 8 inches.
2. The corresponding motion of Structure 2 was about 6 inches.
3. The corresponding motion of Structure 3 was about 5 inches.
4. The structures experienced trivial tilting, less than 0.25° .

A similar summary of the results of electronic instrumentation shows that:

5. The peak vertical downward acceleration of the outer cylinder of the protected structures was always a small fraction of the corresponding free-field acceleration.
6. The corresponding peak accelerations of the inner cylinders were a still smaller fraction of the free-field values.
7. The horizontal displacements were, in general, less than 10 percent of the corresponding vertical displacements.
8. At the 229-psi level (Structures 1 and 2), the relative horizontal displacement between the structures and the soil was of the order of 0.2 inch, which was slightly above the minimum value at which the bottles might be expected to break.
9. At the 104-psi level (Structure 3), the corresponding figure was somewhat less than 0.01 inch. This displacement would not be expected to break the bottles; and since the evidence of the vertical accelerations indicates that they did break, it is believed that their breakage was caused by vertical relative motion.

A similar summary of the results of the excavation shows that:

10. There was no azimuthal dissymmetry in the damage to the frangible elements at either the 104-psi or the 229-psi level.
11. At the 104-psi level, only 25 percent of the bottles were cracked, and it is estimated that only about 5 percent of the available volume was, in fact, filled.
12. At the 229-psi level, it is estimated that 98 percent of the volume was filled.
13. At both locations, there was a momentary compression sufficient to crack bottles beneath the structure, and there was a steady-state expansion of the space beneath the structures.

TABLE 3.1 STRUCTURE MOTION COMPARED WITH FREE-FIELD MOTION, PEAK VALUES

	Vertical				Horizontal			
	Accel (g)		Vel (fps)		Accel (g)		Vel (fps)	
	Down	Up	Down	Up	Out	In	Out	In
	750-ft ground range				229-psi surface overpressure			
Free field	182	23.9	16.2	4.40	0.747	4V1		
5-ft depth	54.7	16.4	15.2	-	0.768	4V5		
10-ft depth	39.2	14.6	10.9	-	0.521	4V10	14.3	5.76 1.42 0.166 0.078 4H10
20-ft depth	46.5	14.3	7.6	-	0.485	4V20A	5.07	2.88 0.865 0.484 0.014 4H50
50-ft depth							11.0	7.08 2.50 0.319 0.098 4HX
Structure 2								
Structure 1								
Outer cylinder	10.0	5.67	6.78	2.09	0.371	4VY1A		
Inner cylinder	1.89	5.14	3.98	2.15	0.400	4VYA	1.73	1.23 0.980 0.271 0.047 4HYA
	1,050-ft ground range				104-psi surface overpressure			
Free field	21.3	8.83	6.13	3.31	0.219	6V1		
5-ft depth	16.8	6.94	6.18	-	0.307	6V5		
10-ft depth								
20-ft depth	9.97	2.62	4.06	0.056	0.293	6V20A	1.31	2.80 0.400 0.128 0.008 6H10
50-ft depth								
Structure 3								
Outer cylinder	5.08	3.38	3.65	1.220	0.184	6VY1A		
Inner cylinder							0.798	0.845 0.303 0.238 0.015 6HYA

TABLE 3.2 RELATIVE PERMANENT HORIZONTAL DISPLACEMENTS OF STRUCTURES

All movements are relative to slab. All measurements are in inches.

Structure Number	Top of Outer Cylinder		Top of Inner Cylinder		Bottom of Inner Cylinder	
	Toward GZ	Away from GZ	Toward GZ	Away from GZ	Toward GZ	Away from GZ
1	$1\frac{1}{8}$		$1\frac{1}{8}$		$\frac{1}{4}$	$\frac{1}{2}$
2	$\frac{7}{8}$		$\frac{1}{2}$		$\frac{1}{2}$	$\frac{5}{8}$
3		$\frac{1}{4}$		$\frac{1}{8}$		$\frac{1}{8}$

TABLE 3.3 PERMANENT VERTICAL DISPLACEMENTS OF SLABS

Structure Number	Range	ft	Downward Displacement
1	750		0.223
2	750		0.161
3	1,050		0.025

TABLE 3.4 RELATIVE DISPLACEMENTS AS SHOWN BY SCRATCH GAGES AND CORK-AND-STRING GAGES

Equivalent stylus motions shown by cork-and-string gages are in parentheses. All measurements are in inches.

Structure Number	Element to which stylus was attached	Element to which paper was attached	Maximum fall of stylus below start	Maximum rise of stylus above start	Final Stylus Position	
					Vertical	Horizontal
			above start	above start	Toward GZ	Away from GZ
1	Slab	Outer cylinder	4.4	3.6	0.71	0.72
	Outer cylinder	Inner cylinder	2.9 ($2\frac{1}{4}$)	0.5 ($\frac{1}{2}$)	0.09 ($\frac{1}{16}$)	
	Slab	Inner cylinder	($6\frac{1}{8}$)	($5\frac{1}{8}$)		($\frac{1}{16}$)
2	Slab	Outer cylinder	2.5 ($2\frac{1}{4}$)	3.9 ($3\frac{11}{16}$)	0.32 ($\frac{1}{16}$)	0.72
3	Slab	Outer cylinder	1.5 ($1\frac{1}{16}$)	3.1 ($2\frac{1}{4}$)	0.04 ($\frac{1}{16}$)	0.03
	Outer cylinder	Inner cylinder	1.1 ($\frac{11}{16}$)	0.3 ($\frac{1}{4}$)	0.16 ($\frac{1}{16}$)	
	Slab	Inner cylinder	(2)	(3)		($\frac{1}{4}$)

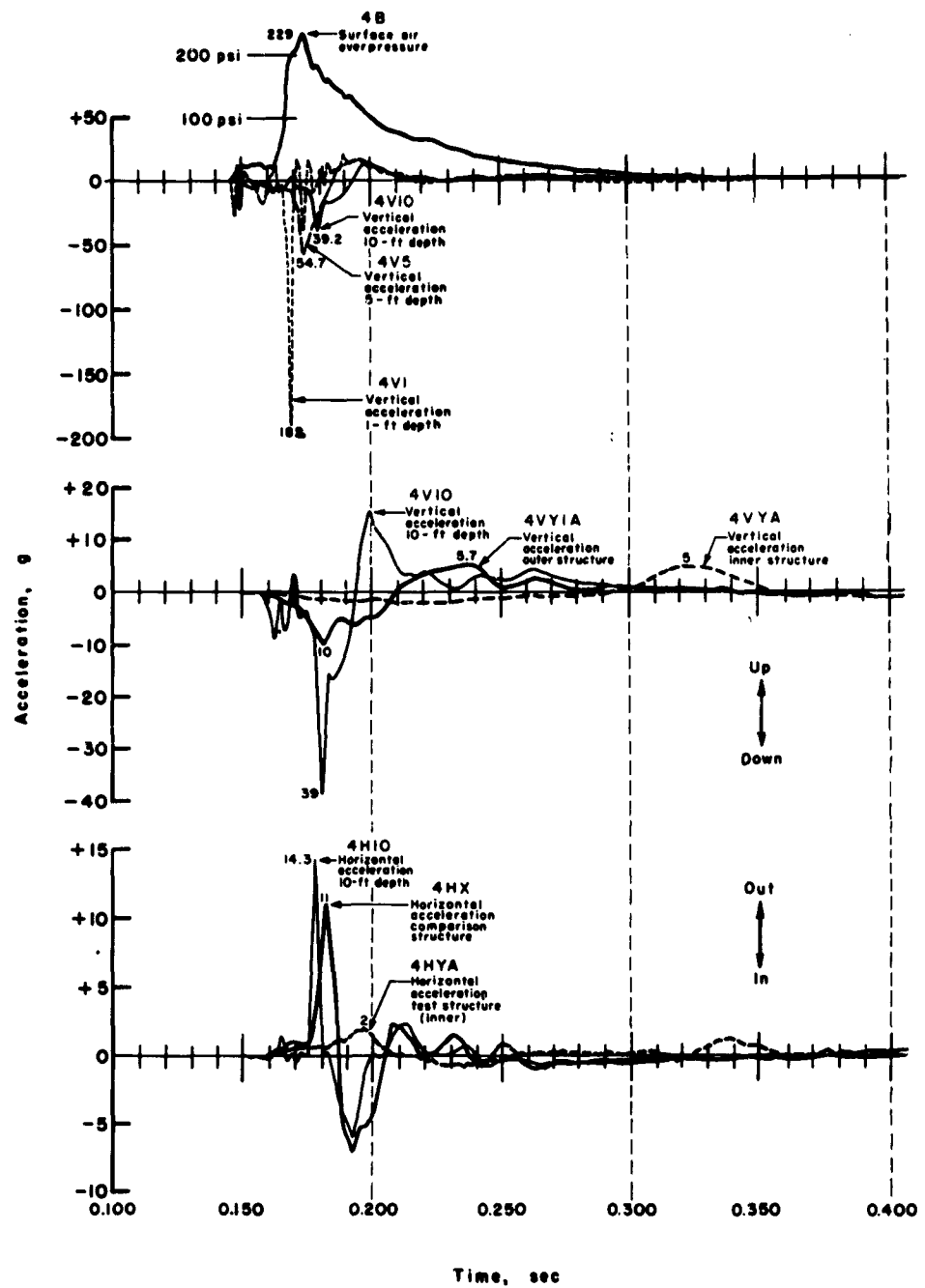


Figure 3.1 Ground and structure acceleration at 229-psi surface overpressure level.

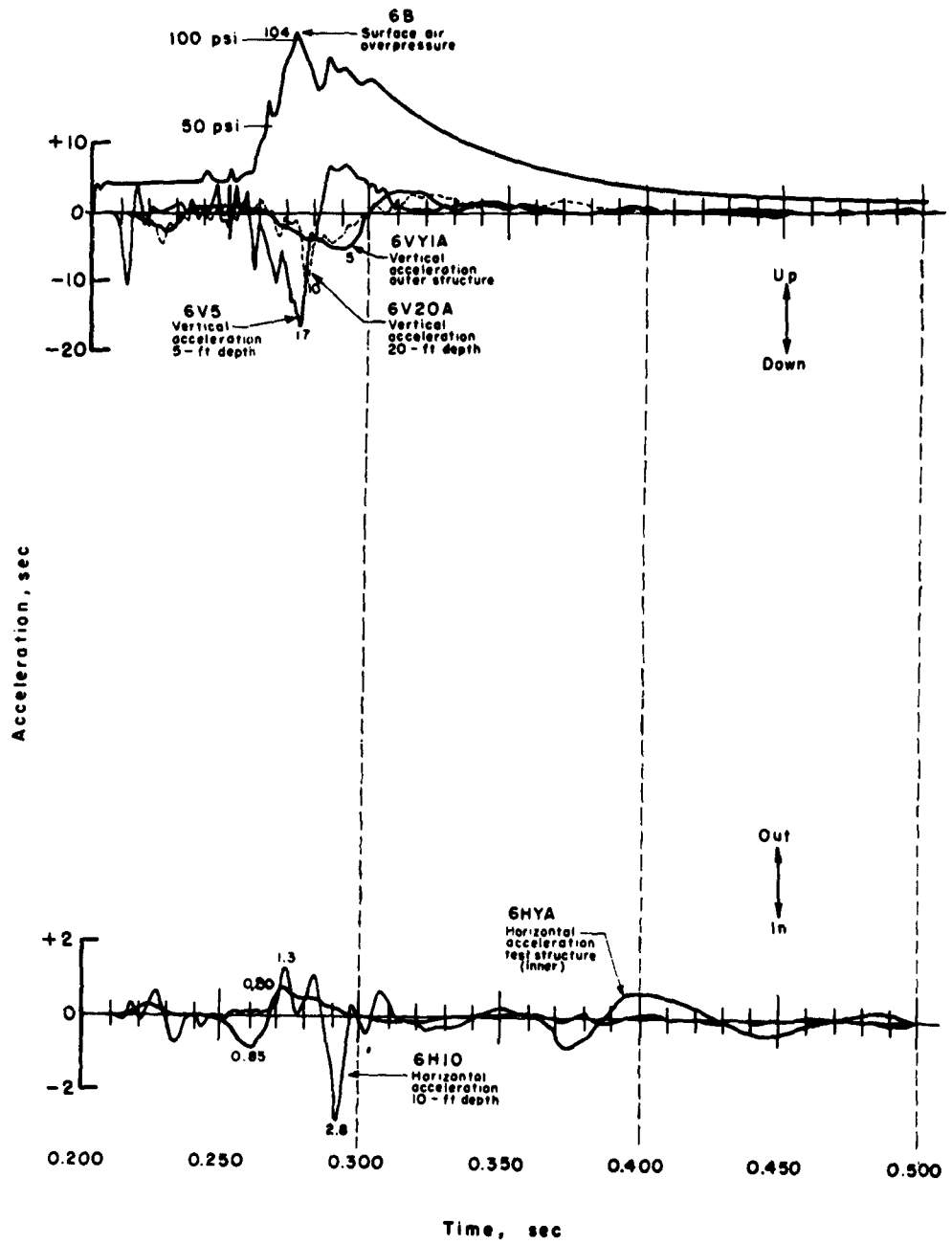


Figure 3.2 Ground and structure acceleration at 104-psi surface overpressure level.

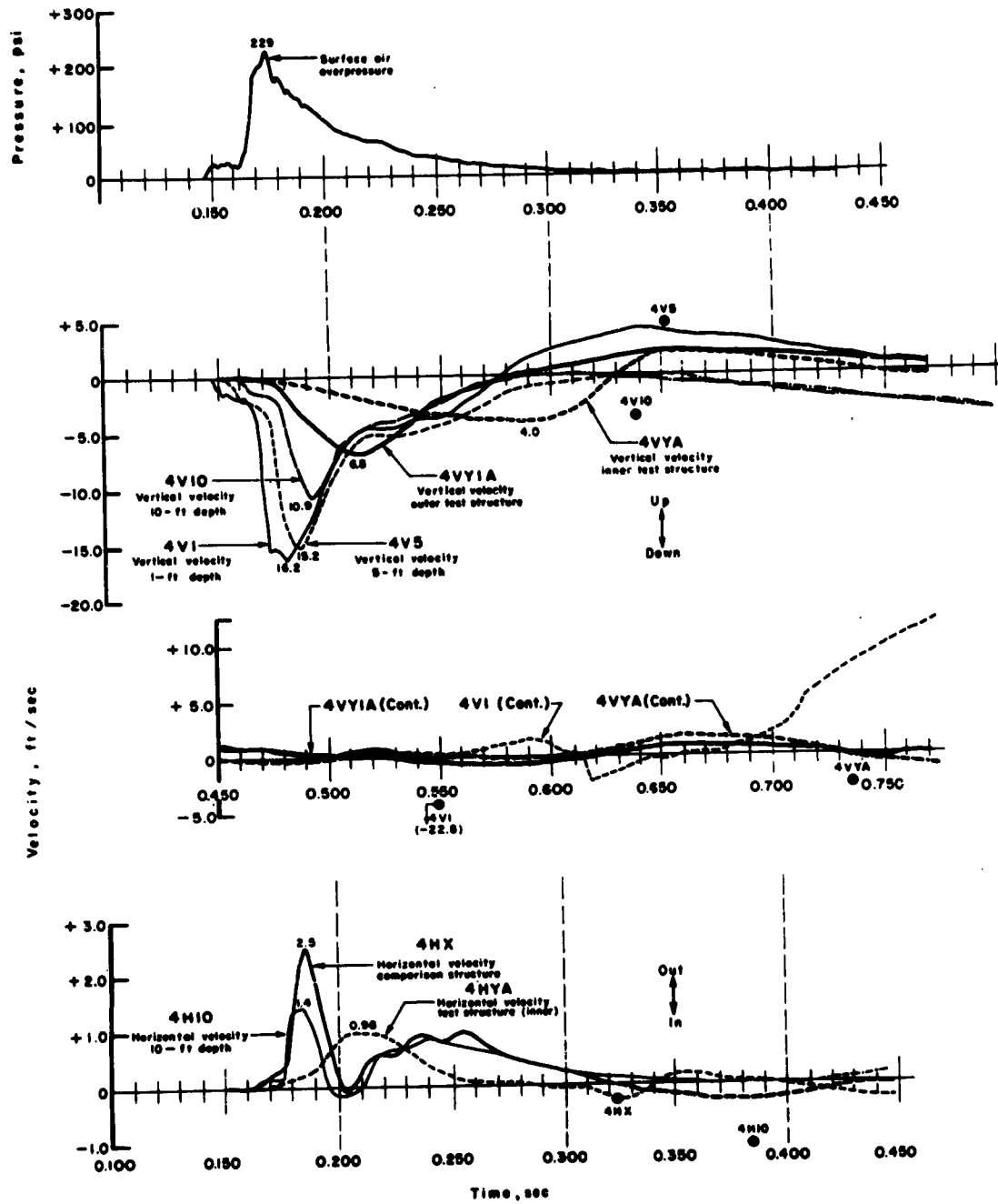


Figure 3.3 Ground and structure velocity at 229-psi surface overpressure level.

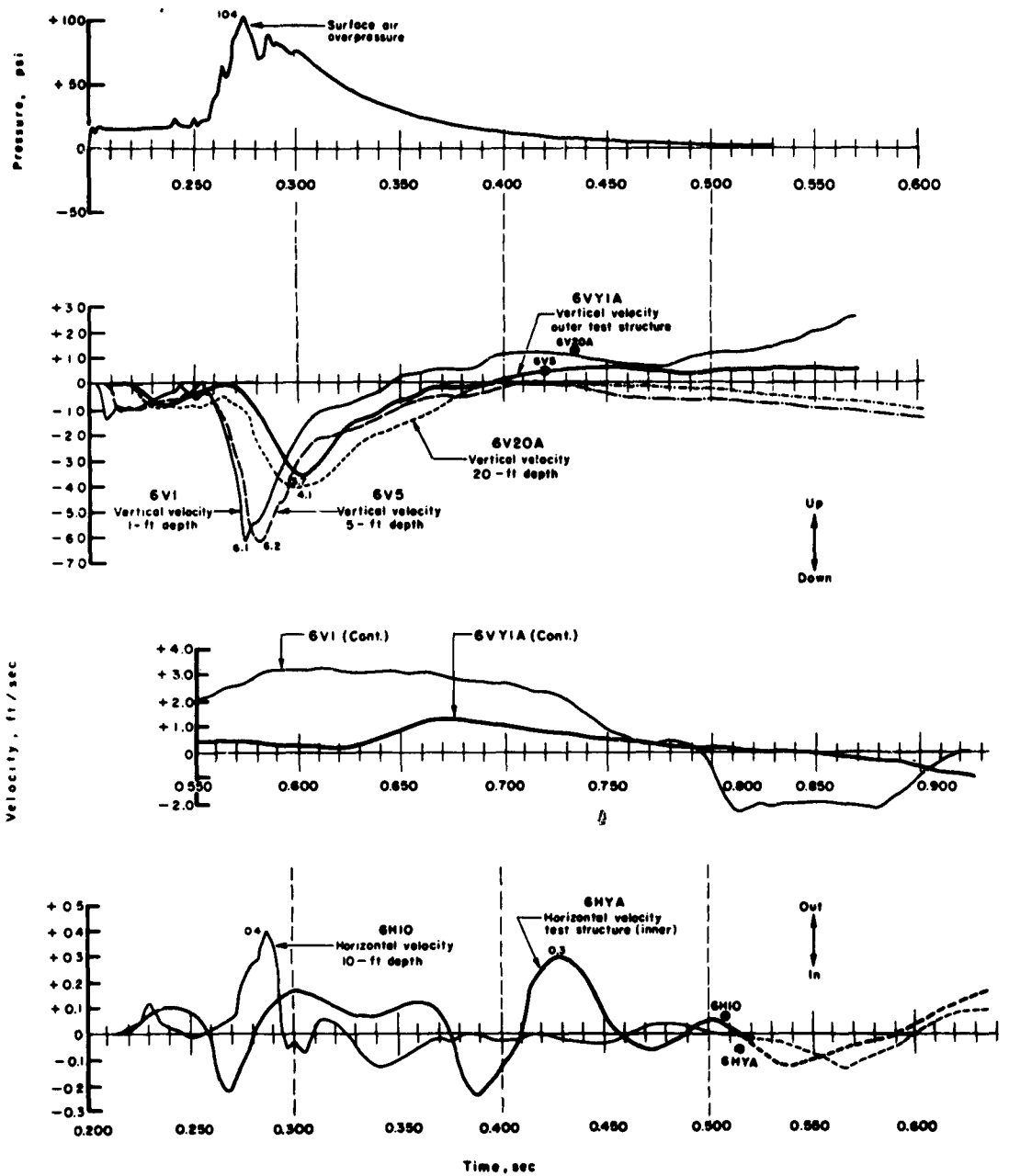


Figure 3.4 Ground and structure velocity at 104-psi surface overpressure level.

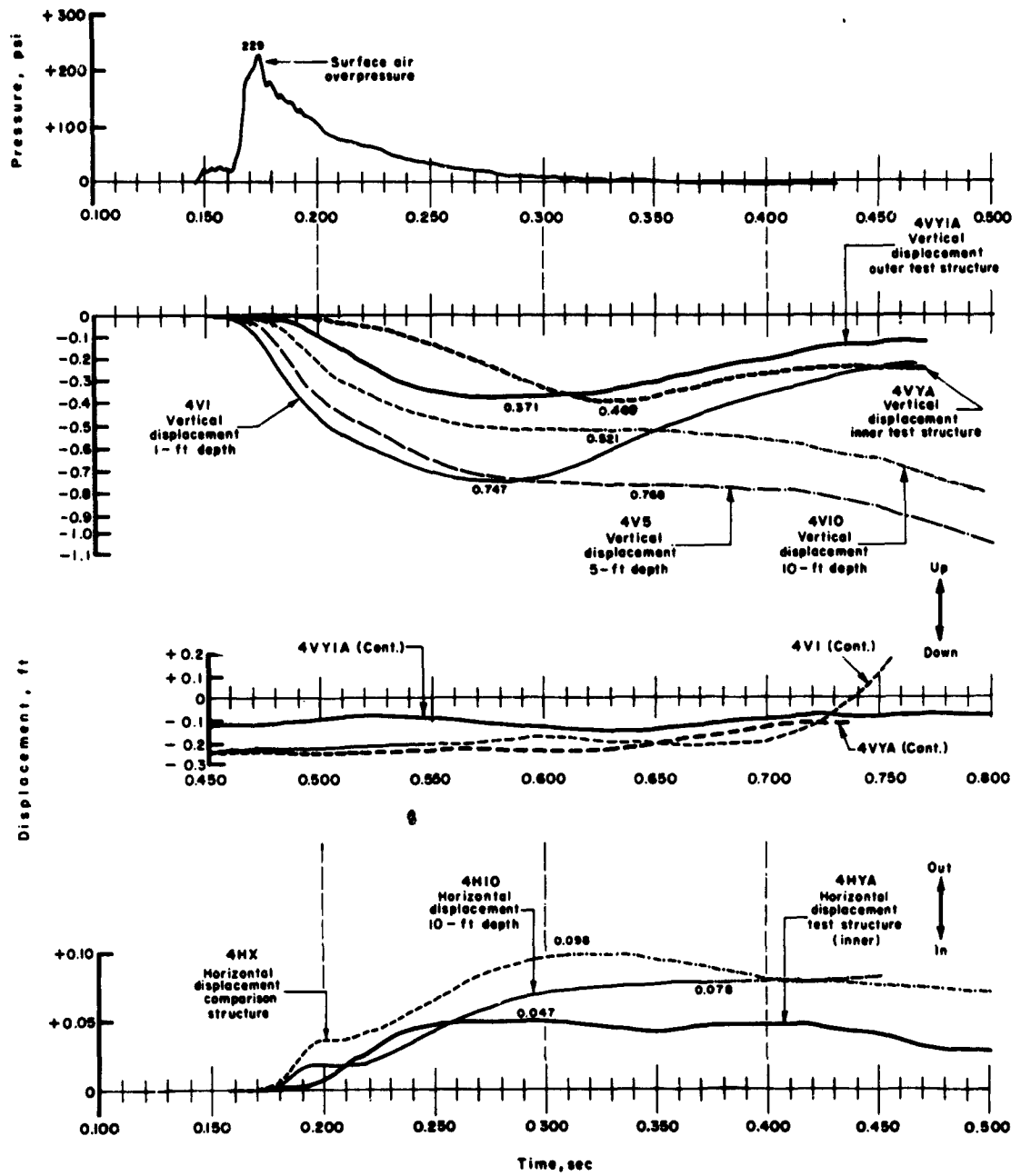


Figure 3.5 Ground and structure displacement at 229-psi surface overpressure level.

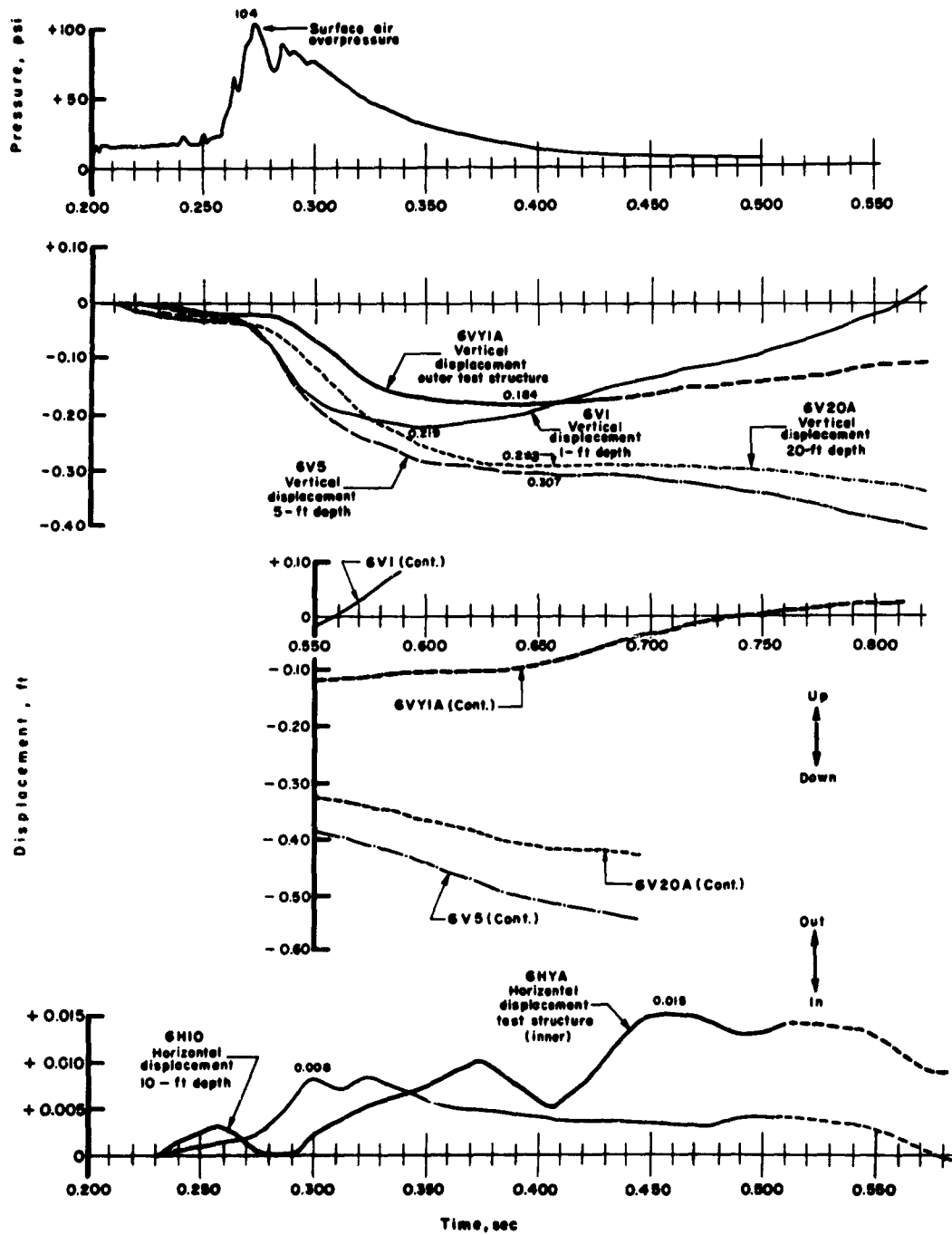


Figure 3.6 Ground and structure displacement at 104-psi surface overpressure level.

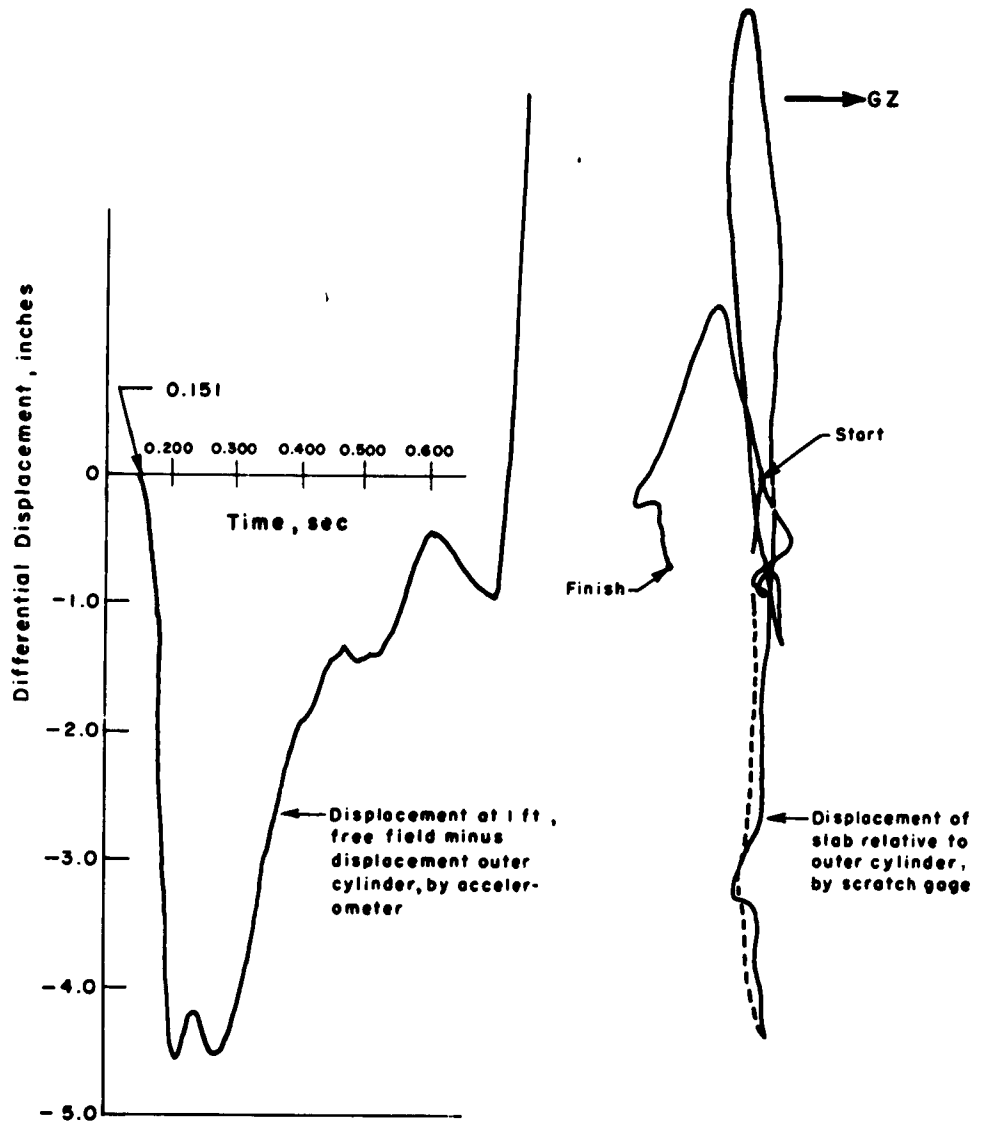


Figure 3.7 Comparison of relative displacements in Structure 1.

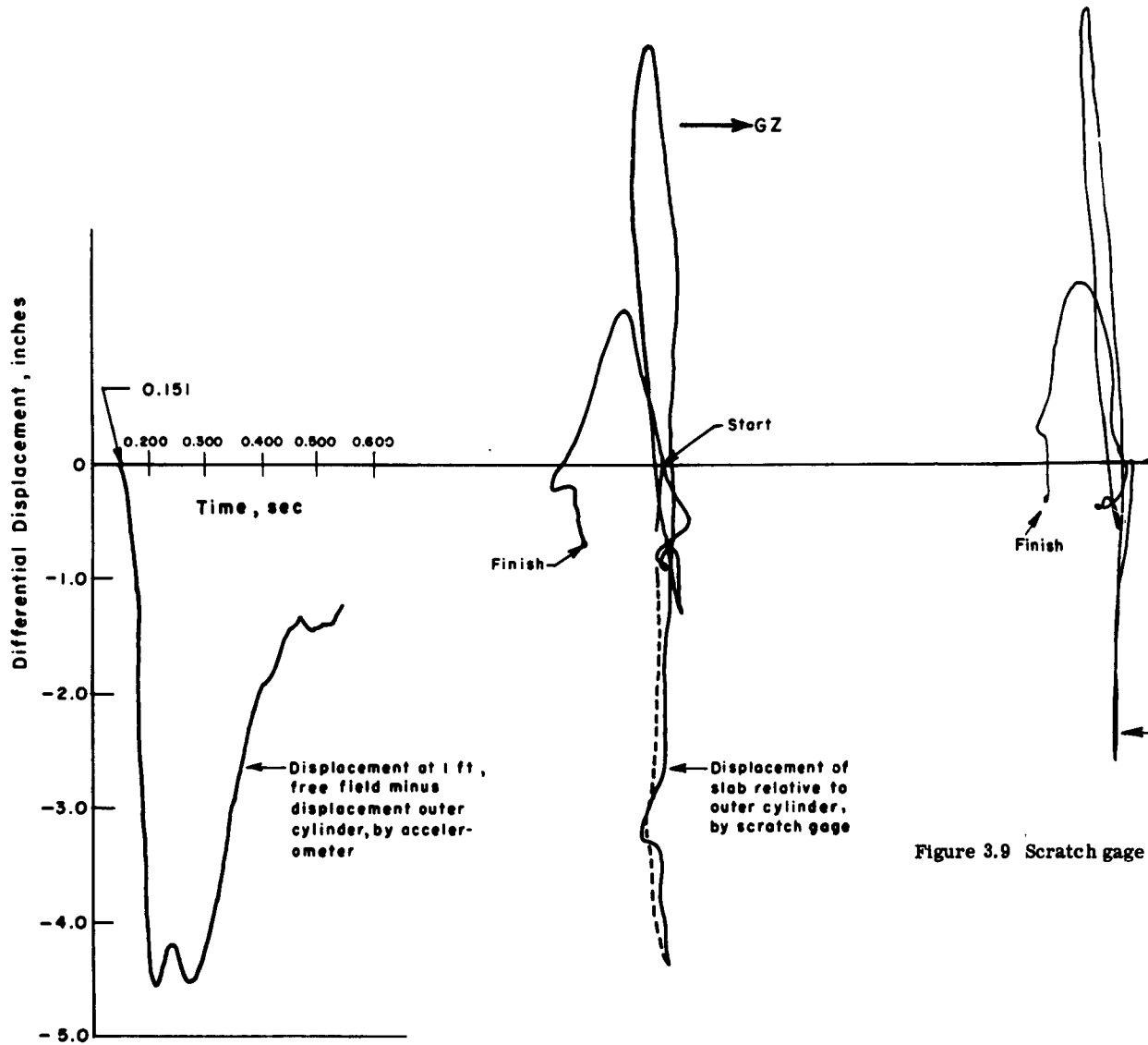


Figure 3.9 Scratch gage

Figure 3.8 Comparison of relative displacements, outer and inner cylinders, Structure 1.

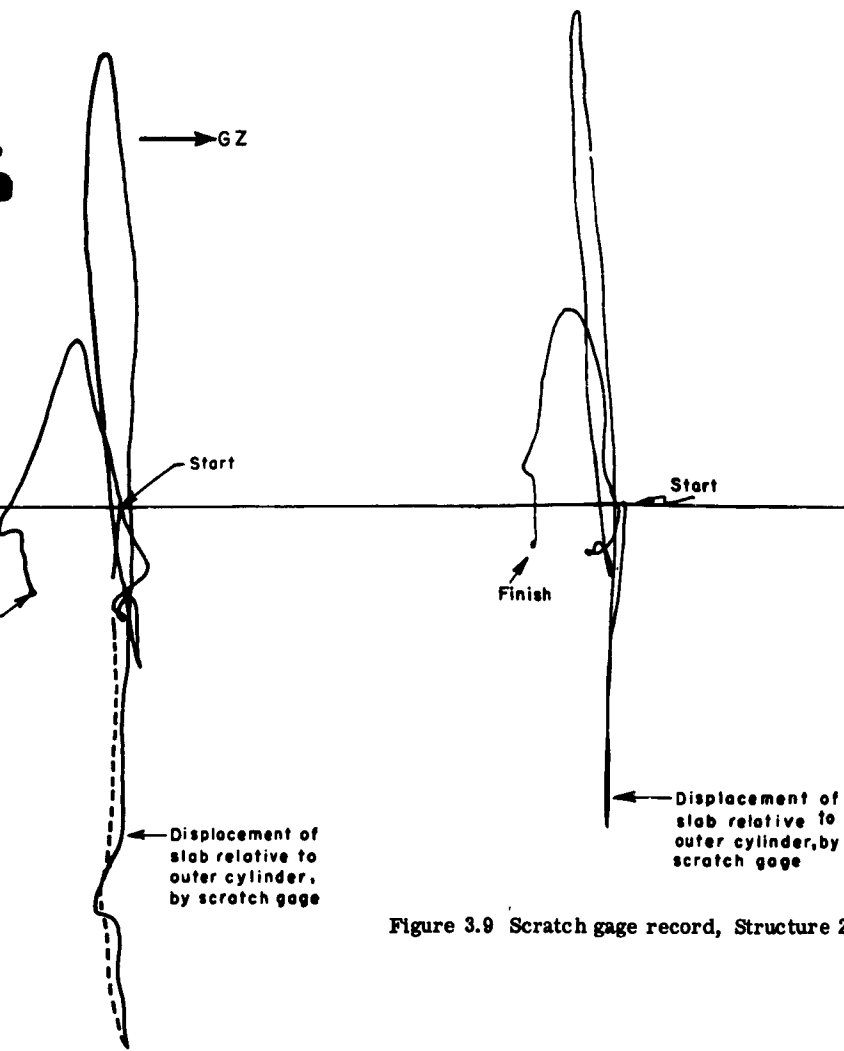


Figure 3.9 Scratch gage record, Structure 2.

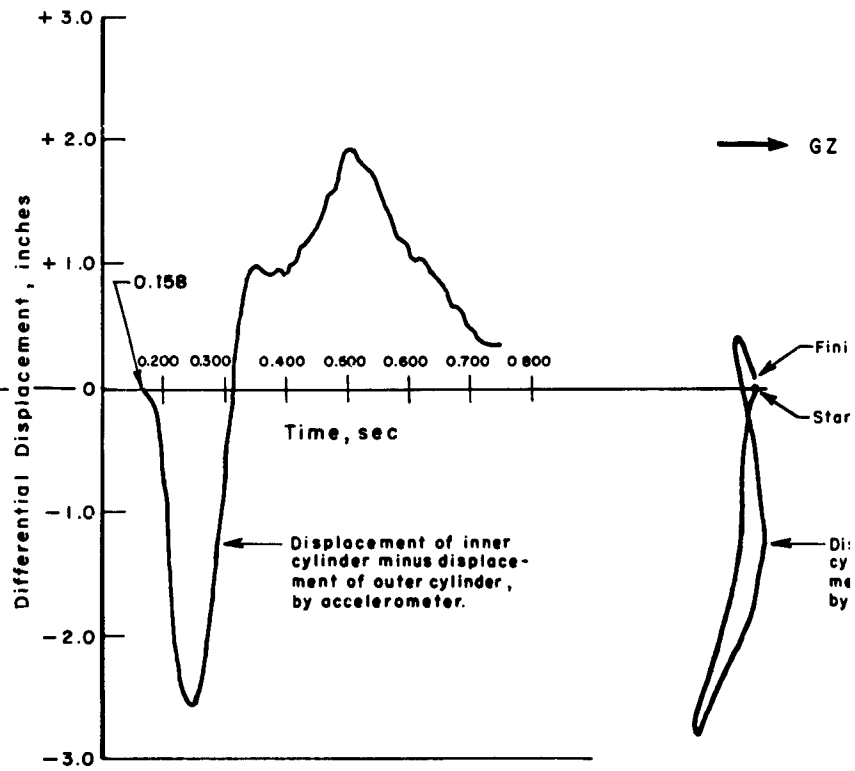


Figure 3.10 Comparison of relative displacements in Structure 3.

placements,

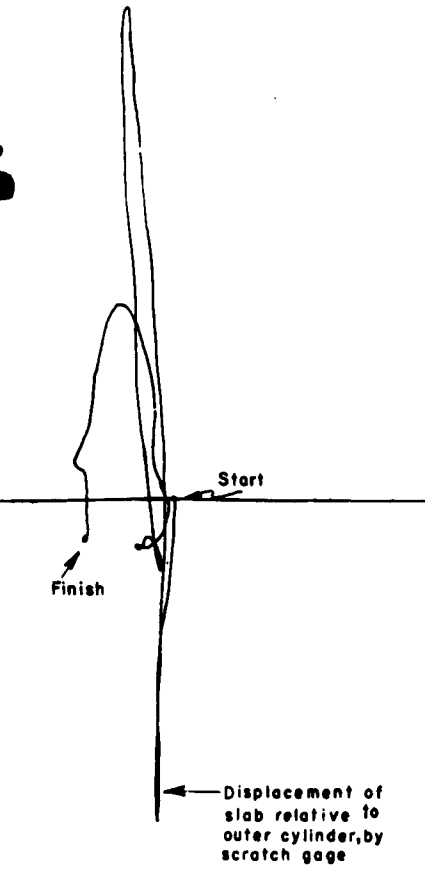


Figure 3.9 Scratch gage record, Structure 2.

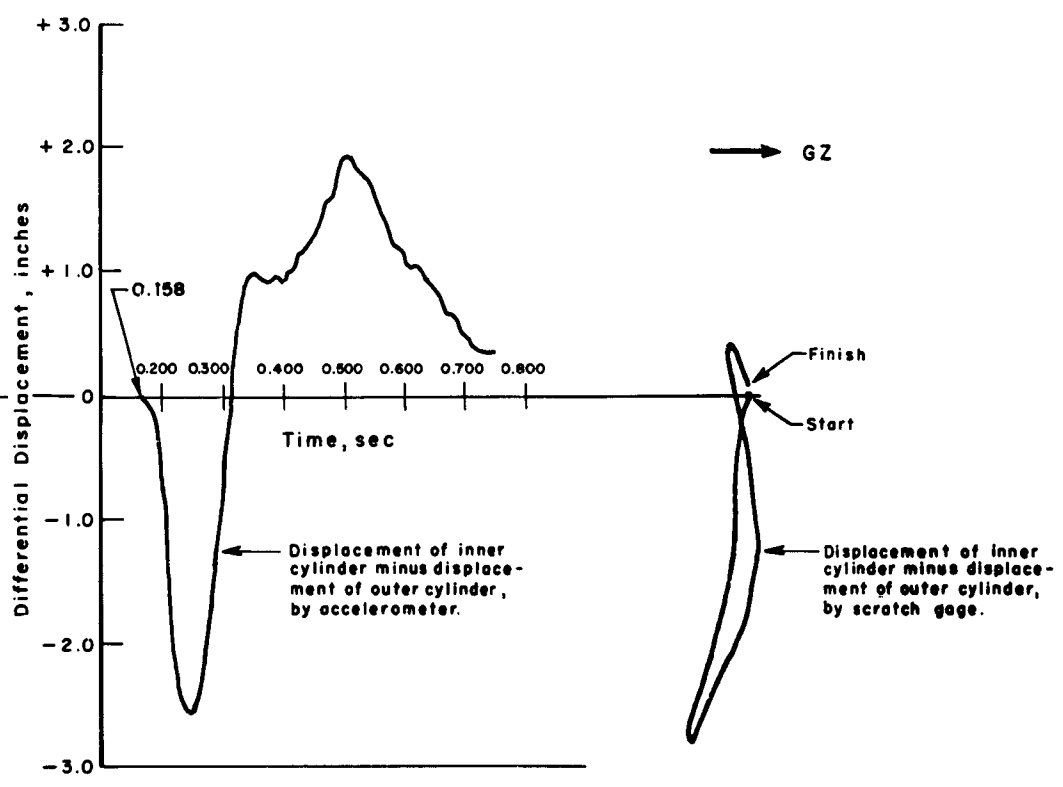


Figure 3.10 Comparison of relative displacements in Structure 3.

3

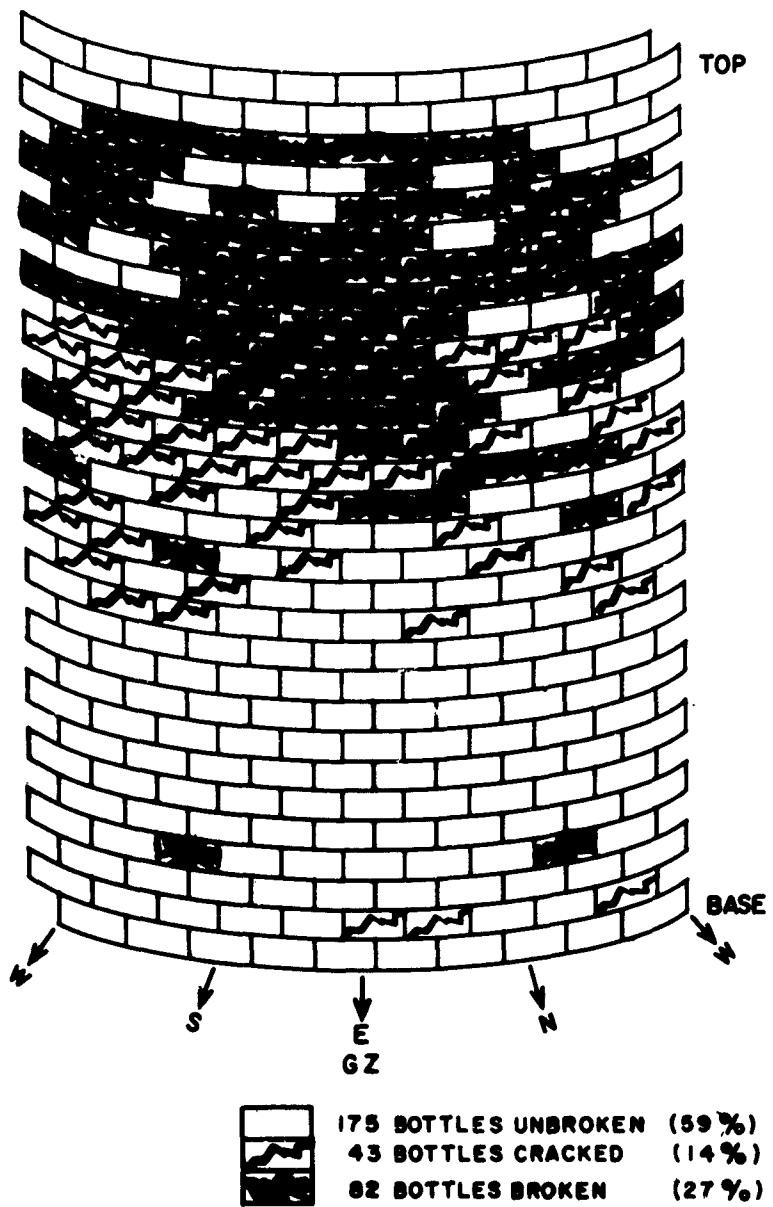
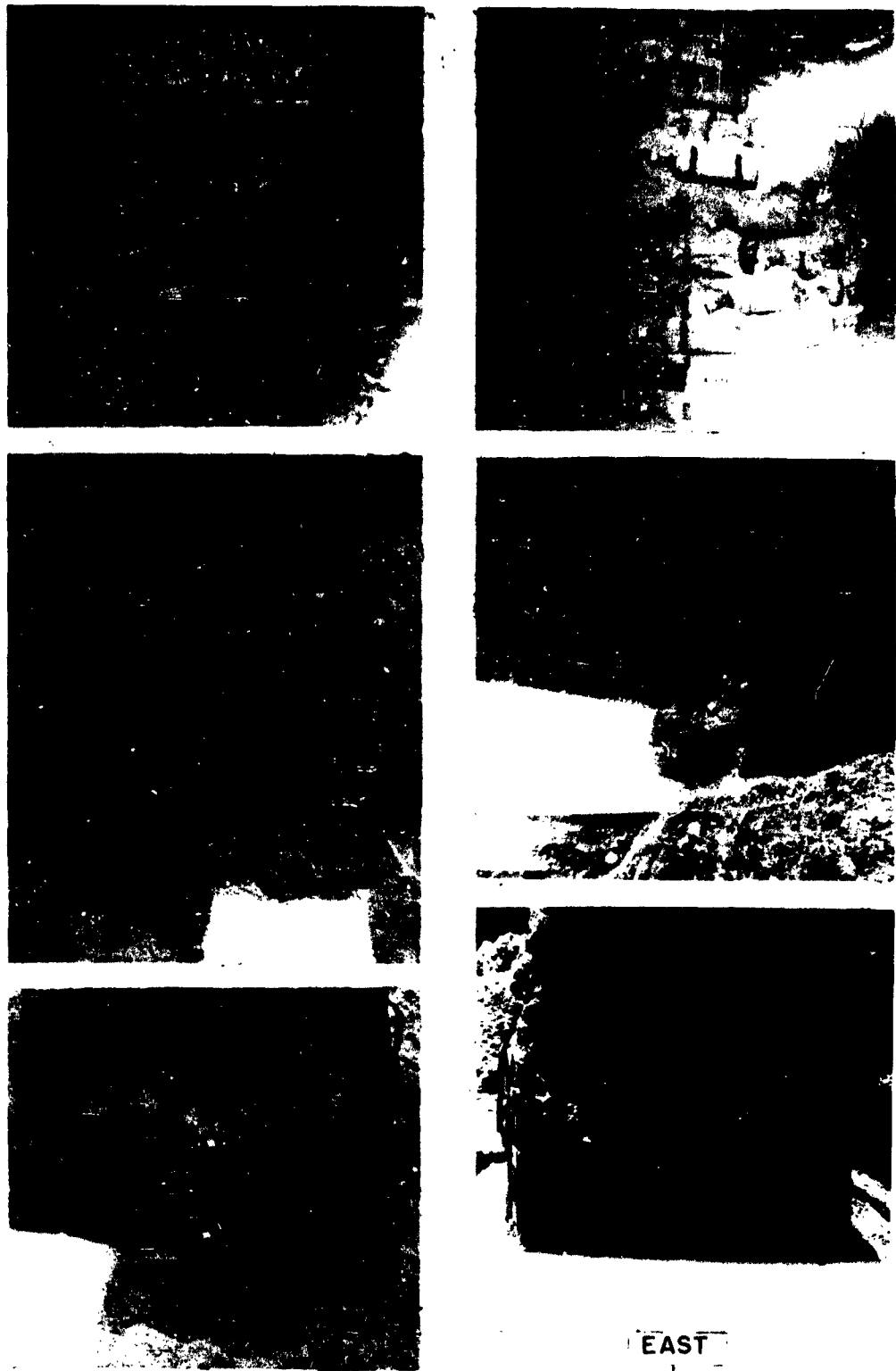


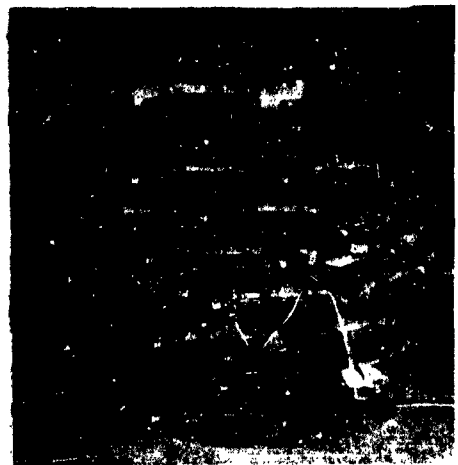
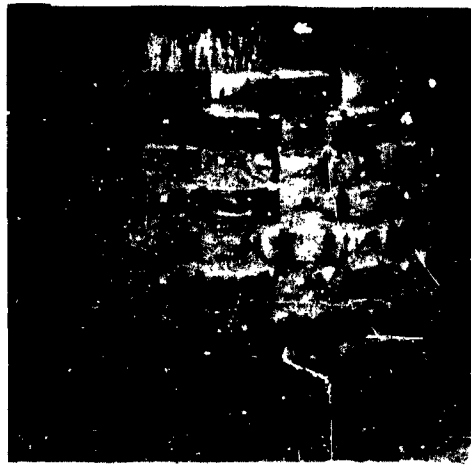
Figure 3.11 Developed surface of excavated Structure 3 indicating condition of bottles.



SOUTH

GROUND ZERO

Figure 3.12 Structure 3 during excavation.



NORTH

WEST

Figure 3.13 Additional views of Structure 3 during excavation.



Figure 3.14 View of Structure 3 showing lateral movement that occurred during excavation.



Figure 3.15 Subbase of Structure 3.



Figure 3.16 Inner subbase of Structure 3 exposed.

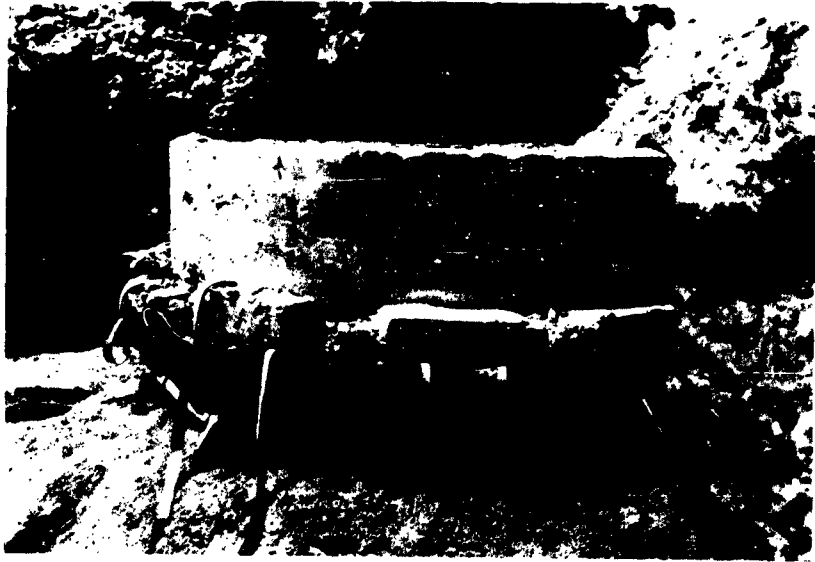


Figure 3.17 Top of Structure 1 as excavated.

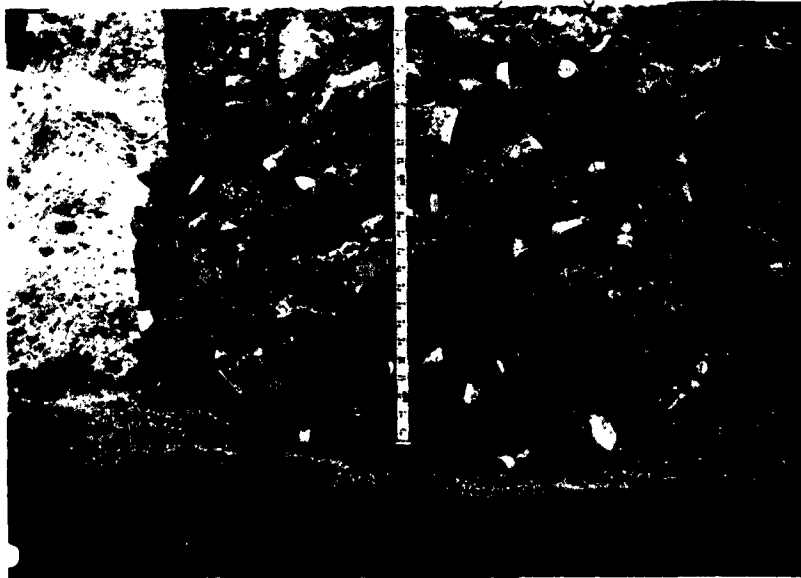


Figure 3.18 Typical condition of bottles attached to Structure 1.

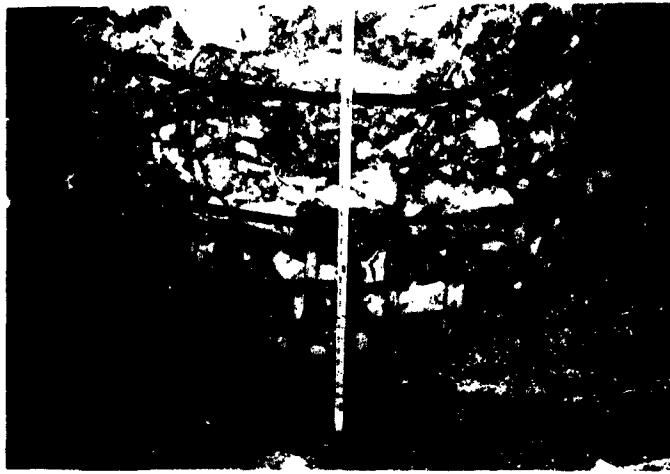


Figure 3.19 View showing bottles in lower part of Structure 1.

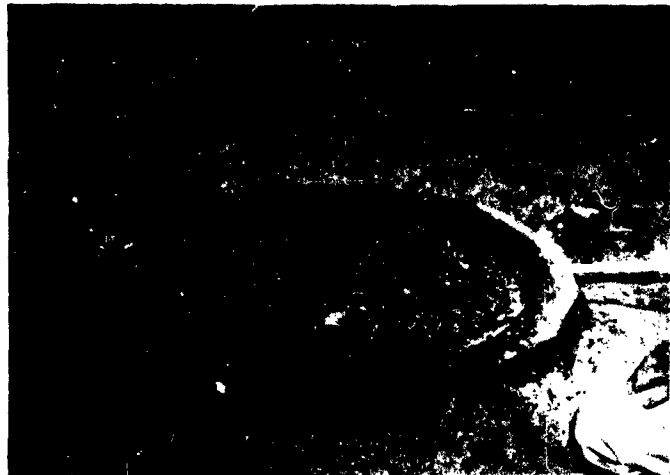
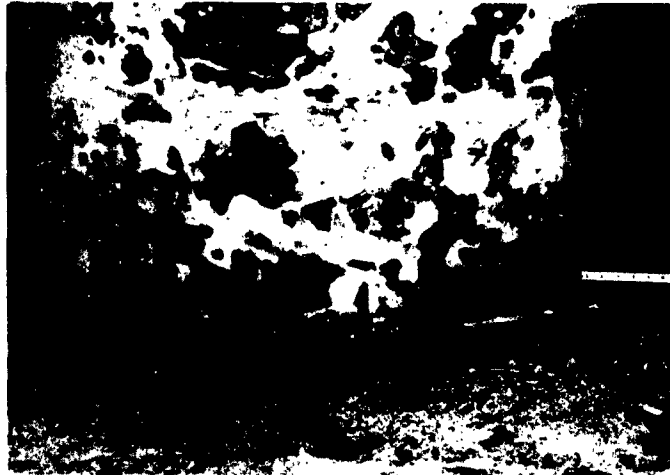


Figure 3.20 View of lower part of Structure 1 showing offset, which occurred during placement, and water damage.

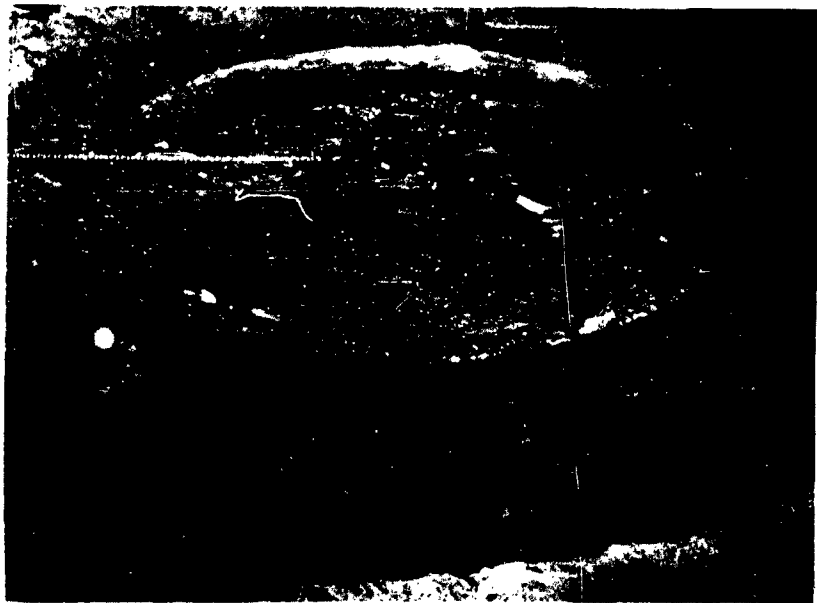
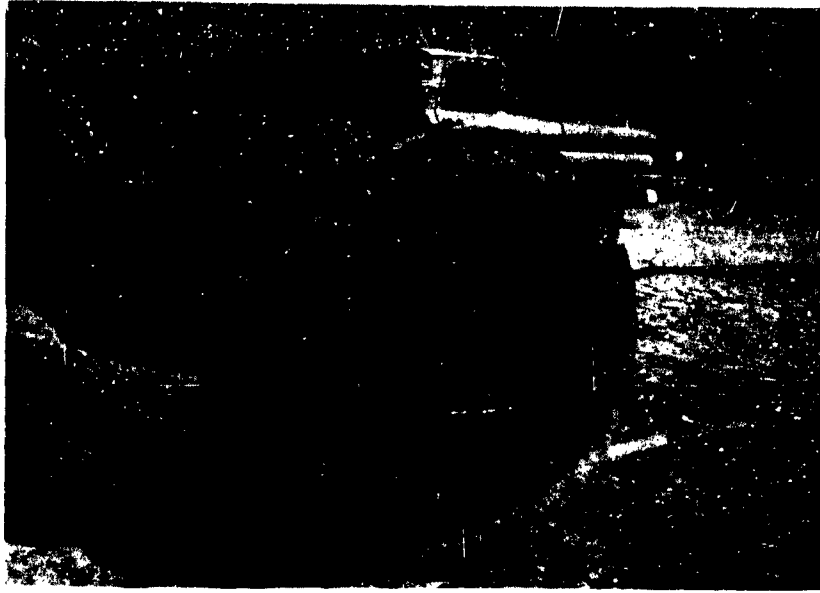


Figure 3.21 Bottom of Structure 1 and subbase showing displaced O-ring.



Figure 3.22 Inner subbase of Structure 1 exposed.

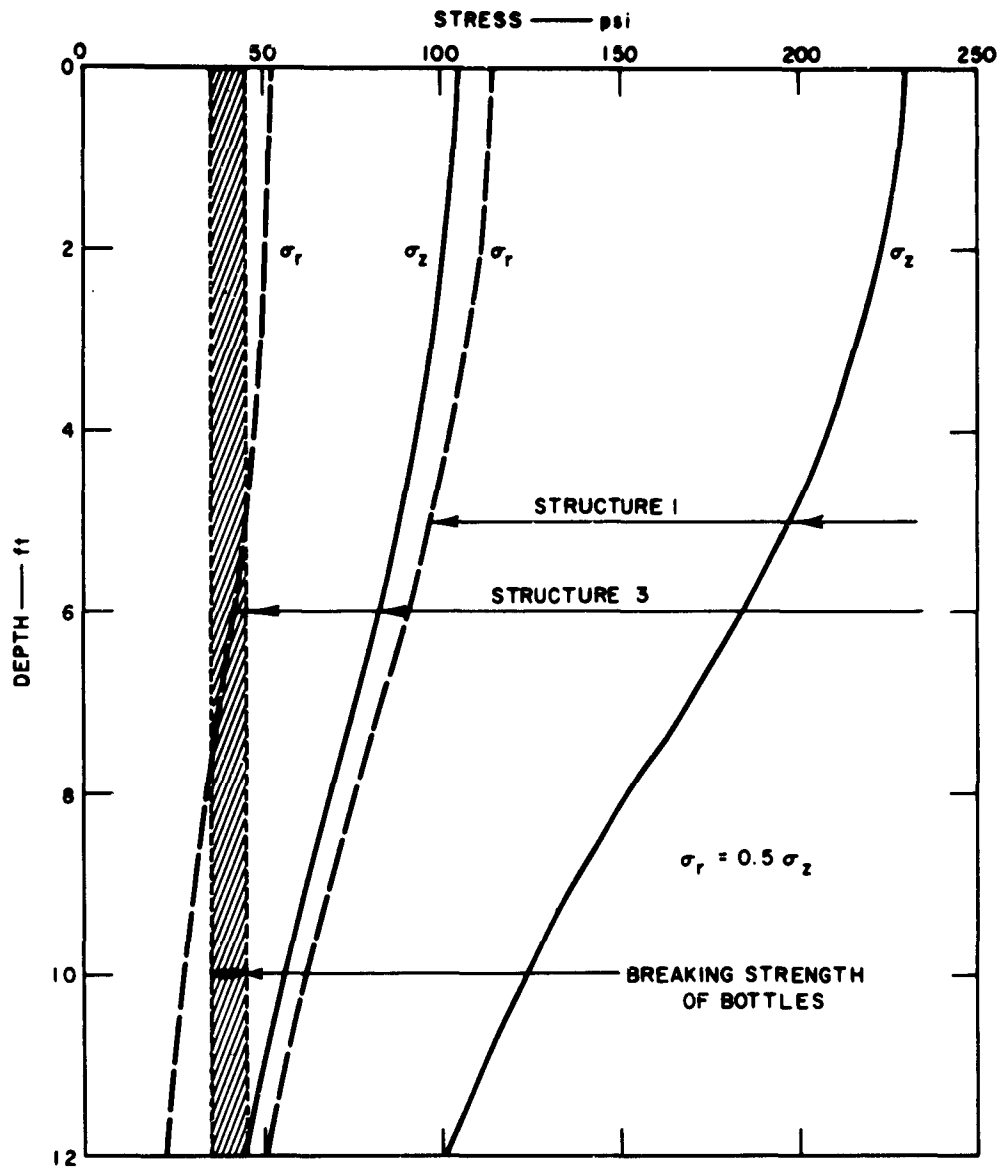


Figure 3.23 Lateral stress as a function of vertical stress.

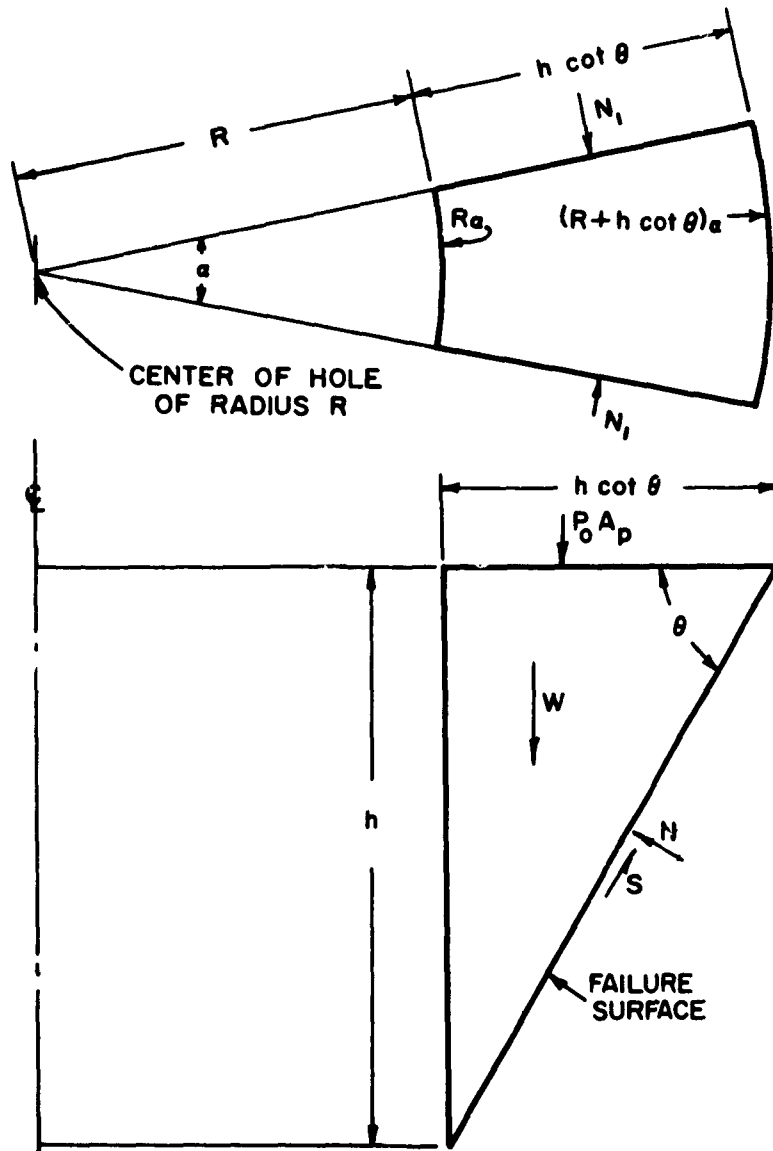


Figure 3.24 Diagram of failure wedge.

Chapter 4

MULTIPLE-ATTACK PROBLEM

The questions — (1) how many attacks should a structure be designed to withstand and (2) how should the design be modified for multiple attack compared with single attack — are very important. On a general basis they are tied up with the efficiency of the diversion of the resources of the country into protective structures. On a specific front, they are of concern in the application of sacrificial protection, such as frangible backfill, because sacrificial backfill enhances the capability of a structure against one attack while leaving unmodified its capability against multiple attack.

The validity of the design of protective construction in withstanding megaton weapons cannot be checked by subjecting the structure to the actual loads, and the direction of enhanced capability is by no means always clear. In addition, the total expenditure of effort and money in protective structures in this country during the next decade may well be a major drain on the economy of the country. In these circumstances it is particularly important to obtain the maximum of protection for every dollar and every man-hour expended in the design and construction of such structures. The situation in protective construction is further confused by the fact that structural engineers commonly operate with factors of safety ranging roughly between 1.5 and 3. To the extent that a factor of safety is precisely known, it is entirely acceptable to the analyst and planner. However, that part of the factor of safety that represents ignorance of the true strength of the structure represents a potentially serious loss of efficiency in the use of funds and effort. Thus, a structure that, for example, begins to show distress at 400 psi can be described as having a factor of safety of 2 against a 200-psi situation or a factor of safety of 1.33 against a 300-psi input. On the other hand, if in a complex of structures designed to withstand an environment of 100 psi, some component structures will be damaged at 150 psi whereas others remain undamaged at 500 psi, then efficiency in the use of funds has suffered. A "one-hoss shay" design is the ideal. (In deference to Dr. Herman Kahn of The RAND Corporation, it is agreed that the first units of any design may appropriately depart from the one-hoss shay ideal; namely, those elements that can be designed for greater strength with very minor additional expense should be so designed, with the presumption that later construction will bring the remainder of the unit up to that increased strength. The one-hoss shay design is ultimately the appropriate one.)

Although the total regime of forces on an underground structure is complex and does not always stem directly from the pressure of the air at the surface above the structure, peak air overpressure is, for the purposes of this discussion, a satisfactory index of the severity of the input to a protective structure.

If structures of steel or of a combination of steel and concrete are subjected to loads of increasing magnitude, for loads below a certain magnitude, the entire structure remains within the elastic range, and when the load is removed, the structure returns to its original condition. Obviously, inputs within this range can be repeated many times without damage to the structure.

Figure 4.1 shows the overpressure as a function of radius together with the probability that, for any one shot, the radius will be greater than the indicated value (peak overpressure from a near-surface burst falls off as the inverse cube of radius R for small r , and as the inverse square for large R). Both curves are normalized to the CEP defined

as the radius within which half the burst points will fall. (There is a tacit assumption that there is no systematic error on the part of the attacker. The conclusions will require some modification if this assumption is seriously in error. This would be the case if, for example, the enemy were mistaken about the geographical location of the target by a distance several times the CEP of his weapons.) Since they both have radius as the abscissa, this parameter can be eliminated and the normalized overpressure can be plotted against probability. This has been done in Figure 4.2, which shows the probability that the actual overpressure for any one shot will be smaller than the indicated value. For convenience, a log scale of normalized overpressure has been used as the abscissa.

In an attack by multiple shots it is clear that (1) any structure can stand a large number of attacks with overpressures lower than that for maximum elastic deflection, and it can be established that (2) the structure can stand no attacks with an overpressure more than twice this large. In the middle range of the curve of Figure 4.2 the probability of occurrence of an overpressure within a 2:1 range is 0.24 and at either end of the curve is still smaller. Therefore, the probability that a structure is damaged but not destroyed by a single shot is 0.24. Only in this 2:1 region, having a probability of 0.24, is the capability of the structure any different for multiple shots than it is for single shots. Now the probability that two attacks will both fall within the same 2:1 pressure span is $(0.24)^2$ or 0.06.

In multiple shots the probability is 0.76 that the shot that produces the maximum overpressure will either destroy the structure or will leave it undamaged. If it destroys the structure, there is no point in considering the other shots of the attack; if it leaves the structure undamaged, none of the other shots will damage the structure and hence they are of no interest. Only in the situation in which the strongest single attack has been in the 2:1 range, which has a probability 0.24, is there any interest in the next strongest shot. The probability that the most severe shot and the next most severe will both fall in the 2:1 pressure range is less than 0.06.

Therefore, when a structure has been designed for a certain capability against a single attack, the additional expenditure justified to protect it against a second attack of the same magnitude is no more than 6 percent. As much as a 24-percent increase in cost may be justified if the strength of the structure against single attack can be doubled. (By doubling the strength against single attack is meant increasing the strength to withstand and attack with twice the peak overpressure.)

These conclusions are essentially independent of the CEP of the attacking weapon or its yield and depend only on the exponent of the pressure-versus-distance curve. This exponent lies between -2 and -3 for the whole range of pressures and distances of practical interest. In addition, although it has been said that the pressure range between maximum elastic load and severe damage is 2:1, in most cases the range is narrower than this. Finally, the S-shape of the curve demonstrates that the probability of an attack with twice the pressure is generally smaller than the maximum value of 0.24, which occurs in the midrange.

For all these reasons the cost justified to double the capability against single attack is less than the 0.24 indicated, and the cost justified for protection against multiple rather than single attack is less than the value of 0.06 given above. The precise mathematical statement is that the justified fractional increase in cost to double the strength of the structure against single attack (C_{2p}) is always less than 0.24, and the corresponding figure (C_m) for protection against multiple attack is less than the square of the actual value of the first.

That is:

$$C_{2p} < 0.24$$

and

$$C_m < C_{2p}^2$$

This says that it is rational to spend four times as much in doubling the protection against single attack as to protect against multiple attack. The pertinence of this conclusion is enhanced because the costs are in fact almost always in the inverse relation. The cost of doubling the strength against one attack is usually less than that of providing for multiple attack. This is particularly true if the increase in strength against a single attack is obtained by the inclusion of a frangible or other sacrificial elements in the backfill.

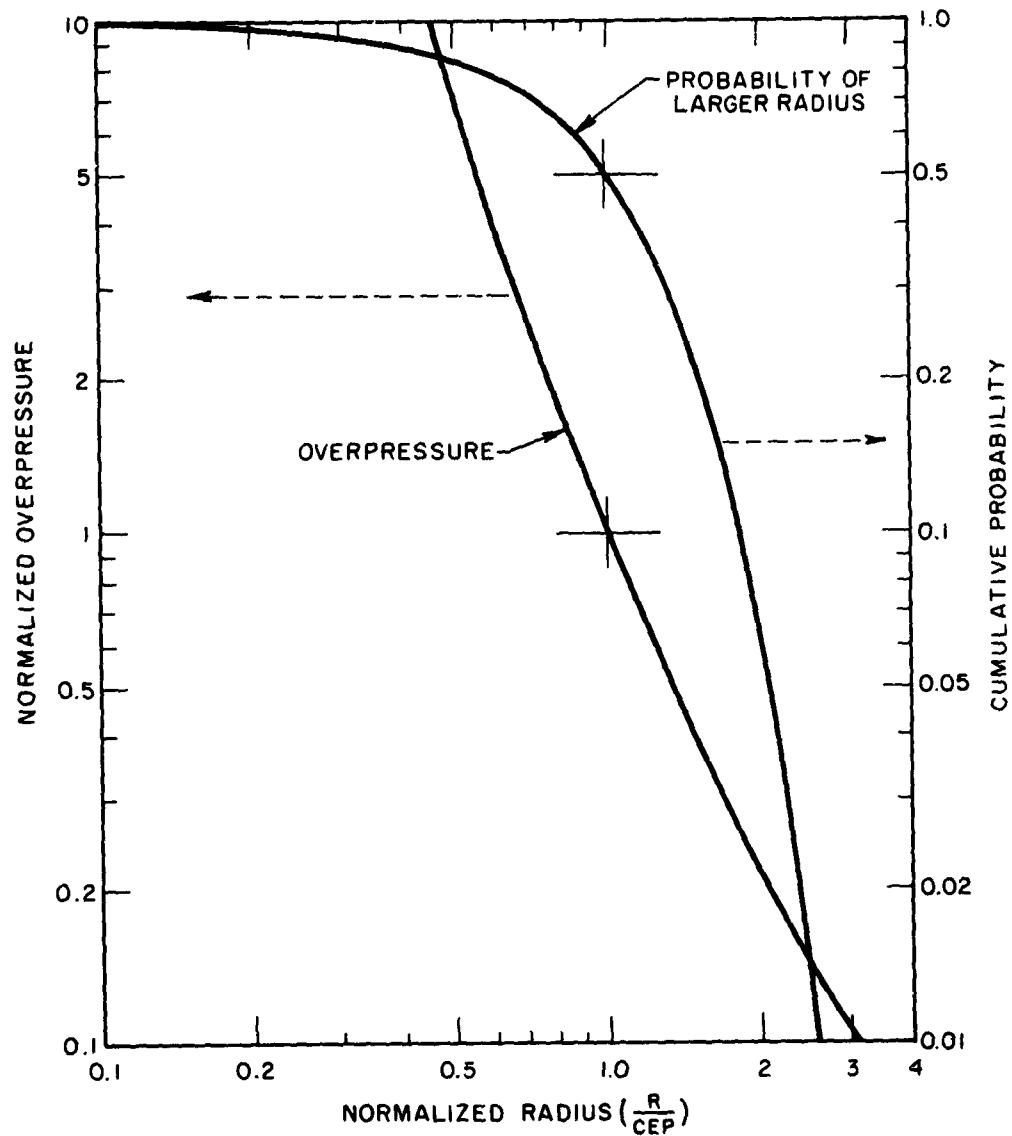


Figure 4.1 Overpressure and probability as a function of radius.

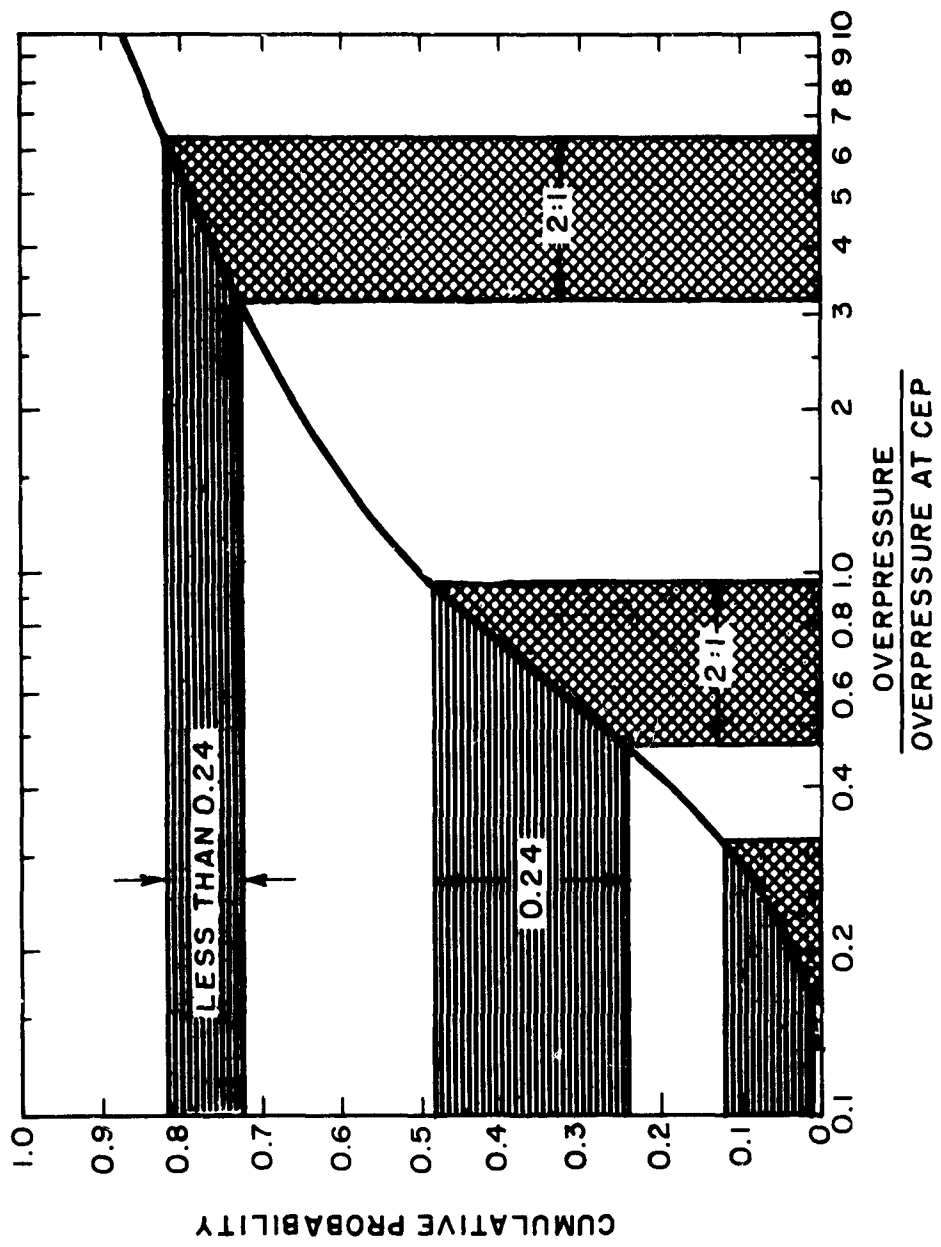


Figure 4.2 Probability versus overpressure.

Chapter 5

CONCLUSIONS AND RECOMMENDATIONS

5.1 CONCLUSIONS

The general conclusion from this experiment is that special backfills offer significant promise in reducing the coupling between underground structures and the surrounding soil and that these backfills are promising even when they are of a sacrificial type. The following specific conclusions are drawn:

1. The peak downward acceleration of the outer part of Structure 1 (229 psi) was 26 percent of the corresponding free-field value at 10-foot depth. The structure acceleration is approximately that which it would have received if it had been unprotected, and placed at a location where the air pressure was half the actual value. This is the best evidence of the value of the frangible elements and sand.
2. The protective capabilities of the frangible elements around Structure 1 were completely used up in this experiment and would not have been available against a second shot. (It should not be inferred that frangible backfill could not have been designed for protection against both this shot and later shots of the same magnitude.)
3. The peak downward acceleration of the inner part of Structure 1 was 21 percent of that of the outer cylinder. This is the best evidence of the value of the rubber O-rings as shear barriers. It suggests promise of lubricant-type shear barriers.
4. The horizontal motion of the inner part of Structure 1 was significantly less than that of the free field at 10-foot depth or of Structure 2 (comparison structure). Since both the frangible backfill and the O-rings acted as compression barriers to horizontal motion, it is not possible to conclude which type of isolation gave the most benefit. The motions were small, and it may well be that the resiliency of the O-rings was a major factor.
5. The peak downward acceleration of the outer part of Structure 3 (104 psi) was less than 50 percent of the corresponding value at 10-foot depth. The acceleration this protected structure actually received was less than it would have received with no protection at the next most distant measuring station at which the air pressure was 60 psi, peak. This describes the value of the frangible elements and sand to this structure.
6. The protective capabilities of the frangible elements were approximately 10 percent expended in the Structure 3 experiment. They would have protected the structure quite effectively against a single second attack at the 200-psi level or against four or five attacks at the 100-psi level.
7. The horizontal motion of the inner part of Structure 3 showed important departures from the motion of the free field at 10-foot depth. These differences were believed to be due primarily to the effect of the O-rings, but the effect of the frangible elements and sand were also included and the two cannot be separated.
8. The horizontal motion of Structure 2 was approximately the same as that of the free field at 10-foot depth.
9. This experiment has demonstrated unequivocally the value of frangible backfill for shallow underground structures. It indicates certain guidelines in further use of frangible structures. It indicates certain guidelines in further use of frangible elements but does not at all define design parameters.

5.2 RECOMMENDATIONS

Capabilities of special backfills of the frangible or sacrificial type merit further investigation in theoretical, laboratory, and field test studies. These studies should include investigation of a variety of backfills and the determination of (1) their properties as shear and as compression barriers, (2) their permeability to water, (3) their tendency to creep, (4) their placement problems, and (5) their cost.

Specific recommendations are as follows:

1. Laboratory tests should be performed to determine the appropriate properties of promising materials. The properties should include compressive stress-strain characteristics under both static and dynamic conditions, and, if possible, shear properties under dynamic inputs. The materials should include foamed materials (plastics and cement concrete) and frangible materials.

2. Analytical studies should be undertaken to outline the range of properties desired and to obtain some indication of the relative importance or value of each. This phase should probably include some specific examples.

3. Field tests should be performed to establish the capability of appropriate materials as compression barriers. The tests should include a megaton shot aboveground. If such a shot is not possible, then the test should be performed by the best simulation available. This may include nonnuclear aboveground explosives or underground nuclear shots. Note that extrapolation from kiloton tests to megaton applications can be accomplished if, but only if, the increased time duration is taken into account.

4. Field tests should be performed to determine the shear capabilities of additional materials and configurations.

5. Frangible sacrificial backfills should be used on current construction of underground protective structures without awaiting the more definitive information to be obtained by further analytical and field studies. This is not to detract from the importance of the tests and studies recommended but reflects confidence that the promise is so great that sacrificial backfills should be used at once. They will enhance the actual level of protection at small cost.

REFERENCES

1. L. M. Swift, et al.; "Ground Acceleration, Stress, and Strain at High Incident Overpressures (U)"; Project 1.4, Operation Plumbbob, WT-1404, May 1960; Stanford Research Institute, Menlo Park, California; Secret Formerly Restricted Data.
2. S. Timoshenko; "Theory of Elasticity"; Second Edition, New York: McGraw-Hill Book Company, Inc., 1951, p. 366.
3. K. Terzaghi; "Theoretical Soil Mechanics"; New York: John Wiley and Sons, Inc., 1943, p. 410.
4. T. B. Goode, et al.; "Soil Survey and Backfill Control in Frenchman Flat"; Project 3.8, Operation Plumbbob, WT-1427, October 1959; U. S. Army Engineer Waterways Experiment Station, Corps of Engineers, Vicksburg, Mississippi; Unclassified.

DISTRIBUTION

Military Distribution Categories 14 and 32

ARMY ACTIVITIES

- 1 Deputy Chief of Staff for Military Operations, D/A, Washington 25, D.C. ATTN: Dir. of SWAR
- 1 Chief of Research and Development, D/A, Washington 25, D.C. ATTN: Atomic Div.
- 1 Assistant Chief of Staff, Intelligence, D/A, Washington 25, D.C.
- 1 Chief of Engineers, D/A, Washington 25, D.C. ATTN: ENRQEB
- 1 Chief of Engineers, D/A, Washington 25, D.C. ATTN: ENRQEB
- 1 Chief of Engineers, D/A, Washington 25, D.C. ATTN: ENRQEB
- 2 Office, Chief of Ordnance, D/A, Washington 25, D.C. ATTN: ORDTM
- 1 Chief of Transportation, D/A, Office of Planning and Int., Washington 25, D.C.
- 3 Commanding General, U.S. Continental Army Command, Ft. Monroe, Va.
- 1 Director of Special Weapons Development Office, Headquarters COMARC, Ft. Bliss, Tex. ATTN: Capt. Chester I. Peterson
- 1 President, U.S. Army Artillery Board, Ft. Sill, Okla.
- 1 President, U.S. Army Air Defense Board, Ft. Bliss, Tex.
- 1 Commandant, U.S. Army Command & General Staff College, Ft. Leavenworth, Kansas. ATTN: ARCHIVES
- 1 Commandant, U.S. Army Air Defense School, Ft. Bliss, Tex. ATTN: Command & Staff Dept.
- 1 Commandant, U.S. Army Armored School, Ft. Knox, Ky.
- 1 Commandant, U.S. Army Artillery and Missile School, Ft. Sill, Okla. ATTN: Combat Development Department
- 1 Commandant, U.S. Army Aviation School, Ft. Rucker, Ala.
- 1 Commandant, U.S. Army Infantry School, Ft. Benning, Ga. ATTN: C.D.S.
- 1 Commandant, U.S. Army Ordnance and Guided Missile School, Redstone Arsenal, Ala.
- 1 Commanding General, Chemical Corps Training Comd., Ft. McClellan, Ala.
- 1 Commandant, USA Transport School, Ft. Eustis, Va. ATTN: Security and Info. Off.
- 1 Commanding General, The Engineer Center, Ft. Belvoir, Va. ATTN: Asst. Cndt, Engr. School
- 1 Director, Armed Forces Institute of Pathology, Walter Reed Army Med. Center, 625 16th St., NW, Washington 25, D.C.
- 1 Commanding Officer, U.S. Army Research Lab., Ft. Knox, Ky.
- 1 Commandant, Walter Reed Army Inst. of Res., Walter Reed Army Medical Center, Washington 25, D.C.
- 1 Commanding General, QM R&D Comd., QM R&D Cntr., Natick, Mass. ATTN: CBR Liaison Officer
- 2 Commanding Officer, Chemical Warfare Lab., Army Chemical Center, Md. ATTN: Tech. Library
- 1 Commanding General, Engineer Research and Dev. Lab., Ft. Belvoir, Va. ATTN: Chief, Tech. Support Branch
- 1 Director, Waterways Experiment Station, P.O. Box 631, Vicksburg, Miss. ATTN: Library
- 1 Commanding Officer, Picatinny Arsenal, Dover, N.J. ATTN: ORDBB-TX
- 1 Commanding Officer, Diamond Ord. Fuze Labs., Washington 25, D.C. ATTN: Chief, Nuclear Vulnerability Br. (230)
- 2 Commanding General, Aberdeen Proving Grounds, Md. ATTN: Director, Ballistics Research Laboratory
- 1 Commander, Army Rocket and Guided Missile Agency, Redstone Arsenal, Ala. ATTN: Tech Library
- 1 Commanding General, White Sands Missile Range, N. Mex. ATTN: ORDBB-OM
- 1 Commander, Army Ballistic Missile Agency, Redstone Arsenal, Ala. ATTN: ORDBB-HT
- 1 Commanding General, Ordnance Ammunition Command, Joliet, Ill.

- 1 Commanding General, U.S. Army Electronic Proving Ground, Ft. Huachuca, Ariz. ATTN: Tech. Library
- 1 Commanding General, USA Combat Surveillance Agency, 1124 N. Highland St., Arlington, Va.
- 1 Director, Operations Research Office, Johns Hopkins University, 6935 Arlington Rd., Bethesda 14, Md.
- 1 Commanding General, U. S. OGD Special Weapons-Ammunition Command, Dover, N.J.
- 1 Commanding General, Southern European Task Force, APO 168, New York, N.Y. ATTN: ACOFS G-3

NAVY ACTIVITIES

- 2 Chief of Naval Operations, D/N, Washington 25, D.C. ATTN: OP-03EG
- 1 Chief of Naval Operations, D/N, Washington 25, D.C. ATTN: OP-75
- 2 Chief of Naval Research, D/N, Washington 25, D.C. ATTN: Code 811
- 3 Chief, Bureau of Naval Weapons, D/N, Washington 25, D.C. ATTN: DLI-3
- 1 Chief, Bureau of Ordnance, D/N, Washington 25, D.C.
- 1 Chief, Bureau of Ships, D/N, Washington 25, D.C. ATTN: Code 423
- 1 Chief, Bureau of Yards and Docks, D/N, Washington 25, D.C. ATTN: D-440
- 1 Director, U.S. Naval Research Laboratory, Washington 25, D.C. ATTN: Mrs. Katherine H. Cass
- 2 Commander, U.S. Naval Ordnance Laboratory, White Oak, Silver Spring 19, Md.
- 1 Commanding Officer and Director, Navy Electronics Laboratory, San Diego 32, Calif.
- 1 Commanding Officer, U.S. Naval Mine Defense Lab., Panama City, Fla.
- 2 Commanding Officer, U.S. Naval Radiological Defense Laboratory, San Francisco, Calif. ATTN: Tech. Info. Div.
- 2 Commanding Officer and Director, U.S. Naval Civil Engineering Laboratory, Port Hueneme, Calif. ATTN: Code L31
- 1 Commanding Officer, U.S. Naval Schools Command, U.S. Naval Station, Treasure Island, San Francisco, Calif.
- 1 Superintendent, U.S. Naval Postgraduate School, Monterey, Calif.
- 1 Officer-in-Charge, U.S. Naval School, CBC Officers, U.S. Naval Construction En. Center, Port Hueneme, Calif.
- 1 Commanding Officer, Nuclear Weapons Training Center, Atlantic, U.S. Naval Base, Norfolk 11, Va. ATTN: Nuclear Warfare Dept.
- 1 Commanding Officer, Nuclear Weapons Training Center, Pacific, Naval Station, San Diego, Calif.
- 1 Commanding Officer, U.S. Naval Damage Control Tug. Center, Naval Base, Philadelphia 12, Pa. ATTN: ABC Defense Course
- 1 Commanding Officer, Naval Air Material Center, Philadelphia 12, Pa. ATTN: Technical Data Br.
- 1 Commander, Officer U.S. Naval Air Development Center, Johnsville, Pa. ATTN: NAS, Librarian
- 1 Commanding Officer, U.S. Naval Medical Research Institute, National Naval Medical Center, Bethesda, Md.
- 1 Commanding Officer and Director, David W. Taylor Model Basin, Washington 7, D.C. ATTN: Library
- 1 Commanding Officer and Director, U.S. Naval Engineering Experiment Station, Annapolis, Md.
- 1 Officer-in-Charge, U.S. Naval Supply Research and Development Facility, Naval Supply Center, Bayonne, N.J.

- 1 Commander, Norfolk Naval Shipyard, Portsmouth, Va. ATTN: Underwater Explosions Research Division
- 1 Commandant, U.S. Marine Corps, Washington 25, D.C. ATTN: Code A03H
- 1 Director, Marine Corps Landing Force, Development Center, MCB, Quantico, Va.
- 1 Commanding Officer, U.S. Naval CIC School, U.S. Naval Air Station, Glynnco, Brunswick, Ga.
- 3 Chief, Bureau of Naval Weapons, Navy Department, Washington 25, D.C. ATTN: RRL2

AIR FORCE ACTIVITIES

- 1 Air Force Technical Application Center, HQ USAF, Washington 25, D.C.
- 1 Hq. USAF, ATTN: Operations Analysis Office, Office, Vice Chief of Staff, Washington 25, D.C.
- 1 Director of Civil Engineering, HQ. USAF, Washington 25, D.C. ATTN: APOCE-ES
- 5 HQ. USAF, Washington 25, D.C. ATTN: AFCIN-3DL
- 1 Director of Research and Development, DCS/D, HQ. USAF, Washington 25, D.C. ATTN: Guidance and Weapons Div.
- 1 The Surgeon General, HQ. USAF, Washington 25, D.C. ATTN: Bio.-Def. Pre. Med. Division
- 1 Commander, Tactical Air Command, Langley AFB, Va. ATTN: Doc. Security Branch
- 1 Commander, Air Defense Command, Ent AFB, Colorado. ATTN: Operations Analysis Section, ADOOA
- 1 Commander, Hq. Air Research and Development Command, Andrews AFB, Washington 25, D.C. ATTN: EDWMA
- 1 Commander, Air Force Ballistic Missile Div. HQ. AFMDC, Air Force Unit Post Office, Los Angeles 45, Calif. ATTN: WDSOT
- 1 Commander, Second Air Force, Barksdale AFB, La. ATTN: Operations Analysis Office
- 2 Commander, AF Cambridge Research Center, L. G. Hanscom Field, Bedford, Mass. ATTN: CRQST-2
- 5 Commander, Air Force Special Weapons Center, Kirtland AFB, Albuquerque, N. Mex. ATTN: Tech. Info. & Intel. Div.
- 2 Director, Air University Library, Maxwell AFB, Ala.
- 1 Commander, Lowry Technical Training Center (TW), Lowry AFB, Denver, Colorado.
- 1 Commandant, School of Aviation Medicine, USAF Aerospace Medical Center (ATC), Brooks AFB, Tex. ATTN: Col. G. L. Hekhuis
- 3 Commander, Wright Air Development Center, Wright-Patterson AFB, Dayton, Ohio. ATTN: WCACT (For WCOSI)
- 2 Director, USAF Project RAND, VIA: USAF Liaison Office, The RAND Corp., 1700 Main St., Santa Monica, Calif.
- 1 Commander, Rome Air Development Center, AFMDC, Griffiss AFB, N.Y. ATTN: Documents Library, RCSBL-1

- 1 Commander, Air Technical Intelligence Center, USAF, Wright-Patterson AFB, Ohio. ATTN: AFCIN-4Bia, Library
- 1 Headquarters, 1st Missile Div., USAF, Vandenberg AFB, Calif. ATTN: Operations Analysis Office
- 1 Assistant Chief of Staff, Intelligence, HQ. USAF, APO 633, New York, N.Y. ATTN: Directorate of Air Targets
- 1 Commander-in-Chief, Pacific Air Forces, APO 953, San Francisco, Calif. ATTN: PFCIS-MS, Base Recovery

OTHER DEPARTMENT OF DEFENSE ACTIVITIES

- 1 Director of Defense Research and Engineering, Washington 25, D.C. ATTN: Tech. Library
- 1 Chairman, Armed Services Explosives Safety Board, DOD, Building T-7, Gravelly Point, Washington 25, D.C.
- 1 Director, Weapons System Evaluation Group, Room 1B880, The Pentagon, Washington 25, D.C.
- 4 Chief, Defense Atomic Support Agency, Washington 25, D.C. ATTN: Document Library
- 1 Commander, Field Command, DASA, Sandia Base, Albuquerque, N. Mex.
- 1 Commander, Field Command, DASA, Sandia Base, Albuquerque, N. Mex. ATTN: FCTO
- 2 Commander, Field Command, DASA, Sandia Base, Albuquerque, N. Mex. ATTN: FCWT
- 1 Commander-in-Chief, Strategic Air Command, Offutt AFB, Neb. ATTN: OAMS
- 1 U.S. Documents Officer, Office of the United States National Military Representative - SSHAPE, APO 55, New York, N.Y.

ATOMIC ENERGY COMMISSION ACTIVITIES

- 3 U.S. Atomic Energy Commission, Technical Library, Washington 25, D.C. ATTN: For DMA
- 2 Los Alamos Scientific Laboratory, Report Library, P.O. Box 1663, Los Alamos, N. Mex. ATTN: Helen Redman
- 5 Sandia Corporation, Classified Document Division, Sandia Base, Albuquerque, N. Mex. ATTN: E. J. Smyth, Jr.
- 10 University of California Lawrence Radiation Laboratory, P.O. Box 808, Livermore, Calif. ATTN: Clovis G. Craig
- 1 Division of Technical Information Extension, Oak Ridge, Tenn. (Master)
- 30 Division of Technical Information Extension, Oak Ridge, Tenn. (Surplus)

ADDITIONAL DISTRIBUTION

- 10 Stanford Research Institute, Menlo Park, Calif.